Tracking the multifield dynamics with cosmological data: a Monte Carlo approach

Journal of Cosmology and Astroparticle Physics
An IOP and SISSA journal

Tracking the multifield dynamics with cosmological data: a Monte Carlo approach

William Giarè,* **Mariaveronica De Angelis, Carsten van de Bruck and Eleonora Di Valentino**

Consortium for Fundamental Physics,
School of Mathematics and Statistics, University of Sheffield,
Hounsfield Road, Sheffield S3 7RH, U.K.

E-mail: w.giare@sheffield.ac.uk, mdeangelis1@sheffield.ac.uk, c.vandebruck@sheffield.ac.uk, e.divalentino@sheffield.ac.uk

Received July 3, 2023
Revised September 27, 2023
Accepted November 5, 2023
Published December 12, 2023

Abstract. We introduce a numerical method specifically designed for investigating generic multifield models of inflation where a number of scalar fields ϕ^K are minimally coupled to gravity and live in a field space with a non-trivial metric $\mathcal{G}_{IJ}(\phi^K)$. Our algorithm consists of three main parts. Firstly, we solve the field equations through the entire inflationary period, deriving predictions for observable quantities such as the spectrum of scalar perturbations, primordial gravitational waves, and isocurvature modes. We also incorporate the transfer matrix formalism to track the behavior of adiabatic and isocurvature modes on super-horizon scales and the transfer of entropy to scalar modes after the horizon crossing. Secondly, we interface our algorithm with Boltzmann integrator codes to compute the subsequent full cosmology, including the cosmic microwave background anisotropies and polarization angular power spectra. Finally, we develop a novel sampling algorithm able to efficiently explore a large volume of the parameter space and identify a sub-region where theoretical predictions agree with observations. In this way, sampling over the initial conditions of the fields and the free parameters of the models, we enable Monte Carlo analysis of multifield scenarios. We test all the features of our approach by analyzing a specific model and deriving constraints on its free parameters. Our methodology provides a robust framework for studying multifield inflation, opening new avenues for future research in the field.

Keywords: inflation, Inflation and CMBR theory, Statistical sampling techniques

ArXiv ePrint: 2306.12414

*Corresponding author.

https://doi.org/10.1088/1475-7516/2023/12/014

JCAP12(2023)014

Contents

JCAP12(2023)014

1 Introduction

Inflation is a period of rapid expansion in the early Universe initially proposed to account for various observational phenomena, including spatial flatness, the horizon and entropy problems, and the apparent lack of topological defects [1–3]. However, it became quickly clear that inflation also offers an elegant mechanism to explain the physical origins of the first fluctuations in the Universe, which eventually gave rise to the observed structures such as galaxies and clusters of galaxies [4–7]. According to the theory of inflation, the initial seeds are generated by quantum fluctuations in the inflaton field (or fields, if inflation is driven by multiple fields) that are stretched to superhorizon scales during inflation, eventually sourcing density fluctuations in other matter species.

Due to its ability to account for the origin of the structures observed in the present-day Universe, inflation is widely accepted as the leading theory of the very early Universe. However, despite its remarkable success, inflation is not free from limitations. From an observational perspective, the absence of a definitive detection of B-mode polarization [8, 9] and the emerging discrepancies among different Cosmic Microwave Background (CMB) experiments [10–18] pose new challenges in determining precise predictions for the inflationary models/mechanisms that best explain observational data [19], and various studies suggest that modifications to the inflationary sector of the cosmological model might play a relevant role in addressing (part of) the tension between the value of the expansion rate of the Universe H_0 [20–24] measured through direct local distance ladder measurements and the value inferred from CMB observations, see e.g., [25–34]. On the other hand, from a theoretical standpoint, despite a plethora of proposed models and mechanisms [35], the nature of the inflation field (or fields) remains still unknown and embedding inflation in a more fundamental theory remains an open problem [36–38].

The simplest dynamical models of inflation involve a single scalar field minimally coupled to gravity whose evolution should be governed by a potential enough flat to induce a phase of slow-roll evolution. However, several non-standard realizations of inflation have been proposed both in the context of extensions to the Standard Model of particle physics and in modified gravity theories and tested against a wide range of available data, including CMB, Big Bang Nucleosynthesis, and Gravitational Wave measurement.[1] Although a large portion of inflation models or theories is predominantly shaped by a single scalar field, low-energy effective field theories inspired by theories of particle physics beyond the Standard Model or quantum gravity, often incorporate multiple scalar degrees of freedom and suggest that inflation could be driven by multiple fields [108], potentially featuring non-minimal couplings [109–124]. When inflation is driven by multiple scalar fields, after the inflationary period, they have to decay into various standard model particles such as dark matter, baryons, neutrinos, and other species. Furthermore, in multifield models, both adiabatic perturbations and isocurvature modes play crucial roles during inflation [125]. These modes can persist immediately after the end of inflation and have a significant impact on the evolution of perturbations during the radiation-dominated epoch, giving rise to a rich phenomenology that can be tested and constrained with cosmological and astrophysical data. Therefore, it is important to extract clues about the period of inflation from cosmological observations to determine at least some of the properties of the field(s) driving inflation in the very early Universe [121, 124–136, 136–163]. In this regard, it is worth noting that both the amount of isocurvature and adiabatic modes can be accurately constrained by recent measurements of the anisotropies and polarization in the cosmic microwave background radiation [164–170], offering a valuable opportunity for experimental validation of multifield inflation. However, obtaining precise predictions from generic multifield models/theories is not always easy because observational quantities often depend on various factors. For instance, it is widely known that different initial conditions for the fields lead to different trajectories in field space which can produce slightly different results for observables such as the amplitude of the scalar and tensor perturbations and the spectral index for scalar perturbations, or isocurvature modes [171]. This makes a comparison between theory and observations more challenging than in single-field inflation, and most tools employed in cosmological data analyses, such as typical Boltzmann integrator codes and samplers, are either unaware of the physics of inflation or assume single-field potentials.[2] As a result, constraining the multifield landscape in light of current observational data represents an ongoing challenge in the field.

In this paper, we take a first step to tackle down this difficulty and introduce a numerical method to precisely calculate the predictions resulting from generic multifield models of inflation where fields are minimally coupled to gravity and the field space metric is allowed to be non-trivial. To this end, our method is made of three key components. First, we numerically solve the complete field equations throughout the entire inflationary period. Once we have ensured that the fields undergo a phase of slow-roll evolution, we numerically solve the background dynamics by adopting a first-order slow-roll approximation and derive predictions for observable quantities such as the spectrum of scalar perturbations, primordial gravitational waves, and isocurvature modes. We also track the behavior of adiabatic and isocurvature modes on super-horizon scales and the transfer of entropy to scalar modes after crossing the horizon using transfer matrix formalism. Secondly, we interface our algorithm with well-known Boltzmann integrator codes and use the inflationary predictions as initial

[1] See, e.g., refs. [11, 35, 39–52, 52–56, 56–58, 58–69, 69–72, 72–107] and references therein.

[2] A few numerical tools for multifield inflation have been developed, as well. See, e.g., ref. [172].

JCAP12(2023)014

conditions to compute the subsequent full cosmology, including the CMB anisotropies and polarization angular power spectra. Finally, we narrow down the viable parameter space of the model and derive constraints on its free parameters by introducing a novel sampling algorithm designed to efficiently explore a large parameter volume and identify regions where predictions agree with observations.

The paper is organized as follows. In section 2, we give an overview of the method, starting with a description of the theoretical parameterization (subsection 2.1), discussing the numerical integration scheme adopted for tracking the multifield dynamics (subsection 2.2), and introducing the sampling algorithm and its interfacing with Boltzmann integrator codes such as `CAMB` [173, 174] or `CLASS` [175] (subsection 2.3). In section 3, we apply this method to an example inflationary model, obtaining constraints on the parameters of the theory. Our conclusions are presented in section 4.

2 Probing the multifield landscape

In this section, we provide a comprehensive overview of the methodology developed for probing the multifield landscape of inflation. In subsection 2.1 we describe the theoretical parameterization adopted for the background equations and the formalism used to track the super-horizon evolution of perturbations. In subsection 2.2 we introduce our integration algorithm, explaining the various analyses performed to reconstruct the multifield dynamics throughout the full inflationary epoch, and the methodology used for calculating observables such as the spectra of primordial scalar and tensor perturbations, and the entropy transfer after horizon crossing. Finally, in subsection 2.3, we explain how our algorithm can be interfaced with standard Boltzmann integrator codes to calculate the subsequent full cosmology of the model and describe the sampling algorithm we designed to explore the parameter-space of generic multifield models and compare theoretical predictions with observations.

2.1 Parametrizing the multifield dynamics

We start by describing generic multifield models where a number of scalar fields ϕ^K are minimally coupled to gravity and live in a field space with a non-trivial metric $\mathcal{G}_{IJ}(\phi^K)$. This geometry is reflected in the kinetic part of the Lagrangian

$$\mathcal{L}_{\rm kin} = -\frac{1}{2}\,\mathcal{G}_{IJ}\nabla_\mu\phi^I\,\nabla^\mu\phi^J. \tag{2.1}$$

Note that in this paper we always work in units $8\pi G = 1$. Considering a spatially flat Friedmann-Lemaître-Robertson-Walker metric, the inflationary dynamics can be described by the generalized Klein-Gordon equations obtained from the variation of the action with respect to the fields ϕ^K:

$$\frac{1}{\sqrt{-g}}\nabla_\mu(\sqrt{-g}\,\mathcal{G}_{IJ}\nabla^\mu\phi^J) = \frac{1}{2}(\nabla_\mu\phi^L)(\nabla^\mu\phi^M)\partial_I\,\mathcal{G}_{LM} - V_{,I}, \tag{2.2}$$

where g is the determinant of the metric tensor, $V \equiv V(\phi^K)$, and the notation $_{,K}$ indicates the derivative with respect to the fields. On the other hand, the evolution of the scale factor $a(t)$ is governed by the Friedmann equations:

$$\begin{aligned} H^2 &= \frac{1}{3}(-\mathcal{L}_{\rm kin} + V(\phi^K)), \\ \dot{H} &= \mathcal{L}_{\rm kin}. \end{aligned} \tag{2.3}$$

JCAP12(2023)014

To facilitate the interpretation of the evolution of linear cosmological perturbations, we adopt the formalism of refs. [176, 177] and perform a rotation in the field space. To do so, we define an orthonormal basis in the field space $\{e_n^I\}$ (with $n = 1, 2$) as

$$e_n^K = \frac{\dot{\phi}^K}{\sqrt{2\mathcal{L}_{\rm kin}}}, \tag{2.4}$$

(where $|\dot{\phi}^K| \equiv \sqrt{2\mathcal{L}_{\rm kin}}$ denotes the length of the velocity vector $\dot{\phi}^K$ containing the fields as components) and the decomposition of their perturbations [178] as

$$E^K = E^n e_n^K. \tag{2.5}$$

In this way, we can introduce the comoving curvature perturbation [176, 178]

$$\zeta = \frac{H}{\sqrt{2\mathcal{L}_{\rm kin}}} E^1, \tag{2.6}$$

which encodes the adiabatic perturbations, as those along the background trajectory e_1^K. It is also worth noting that the whole dynamics of the background fields is encapsulated only in e_1^K and $\dot{e}_1^K$ as $E^K \equiv E^2 e_2^K$ vanishes by construction. In this scenario, the rate of equation (2.6) clearly depends on the entropy perturbations resulting from the presence of the orthogonal fields to the homogeneous trajectory:

$$\dot{\zeta} = \frac{H}{\dot{H}} \frac{k^2}{a^2} \Psi + \frac{H}{\mathcal{L}_{\rm kin}} \left(\mathcal{L}_{,2}\, E^2 \right), \tag{2.7}$$

where $\mathcal{L}_{,2} \equiv e_2^K \mathcal{L}_{,K}$ is the projection of $\mathcal{L}_{,K}$ (i.e., of the derivative of total Lagrangian $\mathcal{L}$ with respect to the fields) on e_2^K (i.e., on the direction of the entropic projection of the field acceleration). Clearly, with the presence of the entropy perturbations, the change of $\dot{\zeta}$ could be significant in addition to the general geometry of the field space.

As previously said, we aim to precisely reconstruct the whole inflationary dynamics and compute the cosmological observables. Therefore, we start by requesting the slow-roll conditions

$$\begin{aligned} \mathcal{G}_{IJ} \dot{\phi}^I \dot{\phi}^J &\ll V(\phi^K), \\ 2\dot{\phi}_I D_t(\dot{\phi}^I) &\ll H\, \mathcal{G}_{IJ} \dot{\phi}^I \dot{\phi}^J. \end{aligned} \tag{2.8}$$

In this regime, we can calculate the primordial scalar spectrum predicted by inflation, evaluated at Hubble radius exit, as

$$\mathcal{P}_\zeta(k) \simeq \left. \frac{H^2}{8\pi^2 c_s\, \epsilon} \right|_{k=k_*}, \tag{2.9}$$

where c_s is the sound speed of the adiabatic perturbation, and

$$\epsilon \equiv -\dot{H}/H^2 \tag{2.10}$$

is the usual slow-roll parameter. Since during the slow-roll phase the expansion rate H is almost constant, we expect the spectrum of primordial perturbations to be almost scale-invariant. Therefore one can expand in terms of the small scale-dependence as

$$\mathcal{P}_\zeta\left(k/k_*\right) = A_s \left(\frac{k}{k_*}\right)^{(n_s-1)+\frac{\alpha_s}{2}\ln(k/k_*)+\frac{\beta_s}{6}\ln^2(k/k_*)}, \tag{2.11}$$

JCAP12(2023)014

where $A_s \equiv \mathcal{P}_\zeta(k_*)$ is the amplitude of the scalar spectrum at the pivot scale $k_\star$, which we fix to $k_\star = 0.05\,\mathrm{Mpc}^{-1}$ throughout this work. In the simplest parameterization any residual scale dependence of the spectrum is parameterized solely in terms of the scalar spectral index n_s defined as:

$$n_s \equiv \left.\frac{\mathrm{d}\ln\mathcal{P}_\zeta}{\mathrm{d}\ln\mathrm{k}}\right|_{k=k_*} = \left.\frac{\mathrm{d}\ln\mathcal{P}_\zeta}{H\mathrm{dt}}\right|_{k=k_*}. \tag{2.12}$$

However, in equation (2.11) we also consider higher-order terms, including the running of the spectral index α_s and its running of running β_s, defined respectively as:

$$\begin{aligned} \alpha_s &\equiv \left.\frac{\mathrm{dn_s}}{\mathrm{d}\ln\mathrm{k}}\right|_{k=k_*} = \left.\frac{\mathrm{d}n_s}{H\mathrm{dt}}\right|_{k=k_*}, \\ \beta_s &\equiv \left.\frac{\mathrm{d}\alpha_\mathrm{s}}{\mathrm{d}\ln\mathrm{k}}\right|_{k=k_*} = \left.\frac{\mathrm{d}\alpha_s}{H\mathrm{dt}}\right|_{k=k_*}. \end{aligned} \tag{2.13}$$

The very same procedure can be repeated for the power spectrum of primordial tensor modes, eventually achieving another useful quantity to constraint general models of inflation, namely the so-called tensor-to-scalar-ratio

$$r \equiv A_T/A_s, \tag{2.14}$$

which quantifies the fraction of primordial gravitational waves produced by the super-adiabatic amplifications of zero-point quantum fluctuations.

Turning our attention to super-Horizon scales, as seen from equation (2.7), once $k^2/a^2 \to 0$, we eventually get

$$\begin{aligned} \dot{\zeta} &= A(t)H(t)\mathcal{S}(t), \\ \dot{\mathcal{S}} &= B(t)H(t)\mathcal{S}(t), \end{aligned} \tag{2.15}$$

with A and B model-dependent functions of time, whose expressions will be explicated in subsection 3.1 for a specific model, and

$$\mathcal{S} = \frac{H}{\sqrt{2\,\mathcal{L}_\mathrm{kin}}}\,E^2, \tag{2.16}$$

a dimensionless gauge-invariant quantity. In order to account for the correlation between curvature and isocurvature modes, as well as to estimate the transfer of entropy from the latter to the former during the time from soon after the Hubble exit to the end of inflation, we make use of the transfer matrix formalism [179]

$$\begin{pmatrix} \zeta \\ \mathcal{S} \end{pmatrix} = \begin{pmatrix} 1 & \mathcal{T}_{\zeta\mathcal{S}} \\ 0 & \mathcal{T}_{\mathcal{S}\mathcal{S}} \end{pmatrix} \begin{pmatrix} \zeta \\ \mathcal{S} \end{pmatrix}_*,$$

where the transfer functions

$$\begin{aligned} \mathcal{T}_{\zeta\mathcal{S}}(t_*,t) &= \int_{t_*}^{t} A(t')H(t')\mathcal{T}_{\mathcal{S}\mathcal{S}}(t_*,t')dt', \\ \mathcal{T}_{\mathcal{S}\mathcal{S}}(t_*,t') &= \exp\left(\int_{t_*}^{t'} B(t'')H(t'')dt''\right), \end{aligned} \tag{2.17}$$

relate the power spectrum at the end of inflation with the power spectrum at the Hubble exit:

$$\mathcal{P}_\zeta = (1+\mathcal{T}^2_{\zeta\mathcal{S}})\mathcal{P}^*_\zeta \equiv \frac{\mathcal{P}^*_\zeta}{\cos^2\Theta}, \tag{2.18}$$

with Θ being defined as the transfer angle.

JCAP12(2023)014

2.2 Integration scheme

After specifying the initial conditions for the fields ϕ^K, their velocities, and the metric $\mathcal{G}_{IJ}(\phi^K)$ of the field space, we can integrate the equations of motion, equation (2.2). The integration process is carried out for a maximum number of e-folds, which is set to $N_{\rm max} = 10000$. During the integration, we dynamically calculate the slow-roll parameter ϵ by equation (2.10) and continue until the condition $\epsilon = 1$ is satisfied. If this condition is not met within $N_{\rm max}$ efolds, the model is rejected as inflation does not end. On the other hand, if the condition is satisfied during integration, the point $\epsilon = 1$ in the parameter trajectory is considered as a possible end of inflation.

To confirm that it represents the actual end of inflation, we check whether the fields are still active enough to begin a second stage of expansion. Specifically, we test whether the normalized field values with respect to their initial conditions do not exceed a threshold value.[3] If the field values satisfy the condition, the multifield dynamics can be considered effectively complete, and the point $\epsilon = 1$ reached during integration is regarded as the actual end of inflation. Instead, if the field values do not meet this condition, the integration continues until they fall below the specified threshold. During this stage, we monitor the value of ϵ to test whether inflation restarts (i.e., if we get back to $\epsilon < 1$). If inflation does not restart, then the original point $\epsilon = 1$ is set as the end of inflation. If inflation does restart, the new end of inflation is determined by the joint conditions of $\epsilon = 1$ and the field values, which must satisfy the selected threshold.[4]

After identifying the end of inflation, we proceed to calculate the total interval of e-fold ΔN between the start of integration and the end of inflation. We make sure that this interval is greater than a threshold value, which we set at $\Delta N \geq 100$. This threshold is crucial to ensure that inflation lasts long enough to account for the observed homogeneity and isotropy of the Universe, and to establish the appropriate initial conditions for the subsequent Hot Big Bang Theory evolution. When the total number of e-folds between the start and end of integration is less than this threshold value, we perform a diagnostic test aimed at determining whether the smaller number of e-folds is due to the initial conditions being chosen too close to the end of inflation or if the model, for that specific combination of parameters, is unable to sustain slow-roll dynamics for an adequate duration. To conduct this test, starting from the same original initial point of integration with the very same initial conditions, we integrate backwards in time from the remaining missing e-folds. During this additional integration, we check the inflationary fields and parameters for any problematic behavior, such as exponentially divergent trajectories, and verify that the model can indeed smoothly support the desired number of e-folds of expansion. If the model fails to meet these requirements, it is deemed unsuitable for explaining the observations and rejected. Note that this test is primarily included to maintain a conservative approach and save a limited number of configurations where models do not respect the threshold value due to the slight shift caused by the random choice of initial conditions while not showing pathological

[3] For the model studied in section 3, we choose $\psi/\psi_{\rm ini} \leq 10^{-3}$ and $\chi/\chi_{\rm ini} \leq 10^{-2}$.

[4] Note that the check detailed in this paragraph is introduced to account for models that exhibit a double inflation behavior, see e.g., refs. [180–190]. Despite in the prototype model studied in section 3 this event appears to be very challenging to realize (i.e., the end of inflation typically corresponds to the conclusion of the field dynamics and does not restart), our code can successfully handle this event, as explicitly discussed in appendix A.

JCAP12(2023)014

behavior of the backward-in-time trajectory. This also reduces the impact on the results from the initial conditions themselves, as argued in section 3.[5]

After ensuring that the model supports a satisfactory number of e-folds of expansion, and having carefully reconstructed the field dynamics during the entire inflationary phase, we can accurately calculate the entire evolutionary history. This includes how the slow-roll parameters and observables evolve as a function of N. By doing so, we can obtain the value of all the slow-roll parameters at horizon crossing, which we choose to be $N_\star = 55$ e-folds before the end of inflation. Additionally, we take into account the evolution on super-Horizon scales and the transfer of entropy to between isocurvature and scalar perturbations. In this way, we can accurately calculate the spectrum of primordial scalar modes (and all the relative observables) at the end of inflation, by means of the transfer matrix formalism detailed in subsection 2.1.

2.3 Sampling method

Once the integration process successfully ends, we can access all the observable predictions of the model, including the amplitude of the scalar perturbation spectrum (A_s), its spectral index (n_s), the scalar running (α_s), the scalar running of running (β_s), and the amplitude of the tensor perturbations (r). To calculate the subsequent cosmology, we interface our algorithm with standard Boltzmann integrator codes. Specifically, we use the "Code for Anisotropies in the Microwave Background" `CAMB` [173, 174].[6] We input the observable predictions of the multifield inflation as initial conditions for `CAMB`, along with any other relevant cosmological parameters, such as the other standard ΛCDM parameters: $\Omega_{\rm b}h^2$, $\Omega_{\rm c}h^2$, $\theta_{\rm MC}$, and τ. This allows us to relate the predictions of the multifield model to the usual observable quantities such as the angular power spectra of cosmic microwave background anisotropies and polarization and the matter power spectrum, in both standard and non-standard cosmological backgrounds.

The next crucial step is to explore the parameter space of generic multifield models by sampling over the initial conditions and the free parameters using Monte Carlo techniques. This enables us to compare the theoretical predictions with observational data and derive observational constraints. To accomplish this goal, we have developed a novel sampling algorithm able to explore a sufficiently large volume of the parameter space and identify a sub-region where the model's predictions agree with observations. Our sampling algorithm works as follows. We input a large number of Monte Carlo steps ($\sim 10^6$ steps). At each step, we randomly select the values of the initial conditions and model parameters within some prior ranges for all sampled parameters. Subsequently, we integrate the model for these initial values, performing all the consistency tests detailed in the previous subsection and keeping only models in which the end of inflation is clearly identified and inflation lasts for a sufficiently long number of e-folds able to explain homogeneity and isotropy. If the model satisfies these initial prerequisites, we calculate the observable predictions for all the inflationary parameters, such as the predicted values of A_s, n_s, α_s, β_s, and r. We then test

[5] In the example studied in section 3, most models are ruled out due to their inability to fit observations for the spectral index and the scalar & tensor amplitudes. The models ruled out because of their inability to sustain a large enough number of e-folds of expansion are the minority, and this is due to the fact that we test from the onset that the fields are settled, so we can safely use the slow-roll approximation when solving the background dynamics.

[6] Note that the very same procedure can be used to interface our algorithm with the 'Cosmic Linear Anisotropy Solving System code', `CLASS` [175].

JCAP12(2023)014

whether these values fall in reasonable ranges, retaining only models that simultaneously satisfies the following conditions:

- $A_s \in [1.5\,,\,2.5] \times 10^{-9}$
- $n_s \in [0.94\,,\,0.99]$
- $\alpha_s \in [-0.2\,,\,0.2]$
- $\beta_s \in [-0.2\,,\,0.2]$
- $r < 0.1$

where we have conservatively chosen the previous ranges around the values measured by the most recent cosmic microwave background experiments.[7] If the model falls within these ranges, we calculate its full cosmology by means of `CAMB`. In this case, we save as output all the relevant information, including the initial conditions, the values parameters, and all observables. If instead the model fails to satisfy any of these conditions, it is rejected.

By following this procedure, we generate a chain of models that are equivalent to those produced by typical Markov Chains Monte Carlo (MCMC) techniques. During the sampling process, each saved model is assigned a likelihood based on how well it agrees with the most recent observations of the Cosmic Microwave Background (CMB). Specifically, our reference datasets include:

- The Planck 2018 temperature and polarization (TT TE EE) data, which also includes low multipole data ($\ell < 30$) [191–193].
- The Planck 2018 lensing data, derived from measurements of the power spectrum of the lensing potential [194].
- The latest CMB B-modes power spectrum likelihood cleaned from the foreground contamination as released by Bicep/Keck Array X Collaboration [9].

To extract a likelihood for each model, starting from these observations we develop an analytical likelihood based on a multi-dimensional normal distribution:

$$\mathcal{L}_{\rm ike} \propto \exp\left(-\frac{1}{2}\left(\mathrm{x}-\mu\right)^{\mathrm{T}}\Sigma^{-1}\left(\mathrm{x}-\mu\right)\right) \tag{2.19}$$

where μ and Σ represent the mean values and covariance matrix of parameters obtained by a joint analysis of the aforementioned experiments. We validate our methodology by verifying that both our analytical likelihood and sampler produce consistent results compared to those obtained by using the original experiment likelihoods and publicly available samplers. We refer to appendix B for further details. Consequently, we can obtain informative posterior distributions for the most relevant parameters to be inferred from observations.

[7] Note that this step is not mandatory, as we could include all models and assign them a likelihood even if they fall outside these ranges. In practice, models following outside these ranges would have a log likelihood of negative infinity and would not contribute to the observational constraints, resulting in identical results. However, when considering large prior volumes, multifield models can exhibit unpredictable outcomes and we may have several models falling outside this range. Therefore, to prevent the evaluation of the likelihood for models known to be disfavored by data, (which would simply slow down the sampling process without changing anything), we introduce this precautionary measure.

JCAP12(2023)014

3 A case study

In this section, we provide a working example of the potentiality of our method. As a case study, we analyze a specific model detailed in subsection 3.1. In subsection 3.2 we demonstrate how our algorithm enables us to track the entire fields dynamics and how we can access all the corresponding observables. Finally, in subsection 3.3, we explore the parameter space of the model by sampling over its free parameters and the initial conditions of the fields, deriving observational constraints.

3.1 Model

We focus on the simple case where two scalar fields $\phi^K = (\psi, \chi)$ are coupled through the field metric

$$\mathcal{G}_{IJ} = \text{diag}\{1, e^{2b(\psi,\chi)}\}, \tag{3.1}$$

and the action reads as

$$\mathcal{S} = \int d^4x\sqrt{-g}\left[\frac{M_{\rm Pl}^2}{2}R - \frac{1}{2}\mathcal{G}_{IJ}g^{\mu\nu}\partial_\mu\phi^I\partial_\nu\phi^J - V(\phi^K)\right], \tag{3.2}$$

where $I, J \in \{1, 2\}$ and g is the determinant of the metric $g_{\mu\nu}$. These models have been recently studied in ref. [124] where it was argued that a non-trivial field metric could induce significant changes in the effective mass of the entropy perturbations, opening up a rich phenomenology that we can test for further validations. For the aim of this section, it is worth noting that the fields dynamics is dictated by equation (2.2) which eventually simplifies to [124]

$$\ddot{\psi} + 3H\dot{\psi} + V_{,\psi} = e^{2b(\psi,\chi)}b_{,\psi}\dot{\chi}^2, \tag{3.3}$$

$$\ddot{\chi} + (3H + 2b_{,\psi}\dot{\psi} + b_{,\chi}\dot{\chi})\dot{\chi} = -e^{-2b(\psi,\chi)}V_{,\chi}. \tag{3.4}$$

By performing a rotation in field space, the evolution of the vector along the homogeneous trajectory (the so-called adiabatic field σ) is given by

$$\ddot{\sigma} + 3H\dot{\sigma} + V_{,\sigma} = 0, \tag{3.5}$$

where $\dot{\sigma} = \sqrt{2\mathcal{L}_{\rm kin}}$. Instead, the entropy part of the equations of motion is given by the rate of change of the angle between the initial field basis (ϕ, χ) and the adiabatic/entropy one (σ, s):

$$\dot{\theta} = -\frac{V_{,s}}{\dot{\sigma}} - b_{,\psi}\dot{\sigma}\sin\theta. \tag{3.6}$$

To consistently discuss the perturbations of a given cosmological configuration, we take into account the perturbations of the metric $\Phi = \Phi(t, \mathbf{x})$ in the longitudinal gauge [195]

$$ds^2 = -(1 + 2\Phi)dt^2 + a^2(t)(1 - 2\Phi)d\mathbf{x}^2, \tag{3.7}$$

and the corresponding fluctuations of the sources such as $\psi = \psi(t) + \delta\psi_{\mathbf{k}}(t, \mathbf{x})$ and $\chi = \chi(t) + \delta\chi_{\mathbf{k}}(t, \mathbf{x})$. By considering equation (3.7) and the perturbed Einstein equations, we write the comoving curvature perturbation equation (2.6) in terms of the metric fluctuations as [124]

$$\zeta \equiv \Phi - \frac{H}{\dot{H}}(\dot{\Phi} + H\Phi) = \Phi + H\left(\frac{\dot{\psi}\delta\psi + e^{2b}\dot{\chi}\delta\chi}{\dot{\psi}^2 + e^{2b}\dot{\chi}^2}\right), \tag{3.8}$$

JCAP12(2023)014

and its evolution as

$$\dot{\zeta} = \frac{k^2}{a^2}\frac{H}{\dot{H}}\Phi - 2\frac{V_{,s}}{\dot{\sigma}}\mathcal{S}, \tag{3.9}$$

where $\mathcal{S} = \frac{H}{\dot{\sigma}}\delta s$ is the so-called isocurvature perturbation, a gauge-invariant quantity. Note that from equation (2.16) it follows that $E^2 = \delta s$. Clearly, the quantity labeled as adiabatic perturbation equation (3.9) on super-Hubble scales (i.e. $k^2/a^2 \to 0$) is solely fed by the entropy perturbation δs, namely by the orthogonal field to the background trajectory in field space. Indeed, even if the perturbations in the entropy field evolve independently from the perturbation in the adiabatic field, the large-scale entropy perturbations do impact the evolution of the adiabatic one when the value of the potential curvature is non-zero, i.e. $\eta_{,\sigma s} \neq 0$. Furthermore, their coupling (encoded in the term $V_{,s}$) does not vanish even when a flat field metric is considered. In other words, $\dot{\theta} \equiv 0$. For this model, the time-dependent dimensionless functions A and B in the transfer function, equation (2.17) are [124]

$$\begin{aligned} A &= -2\eta_{,\sigma s} + 2\sqrt{2\epsilon}b_{,\psi}\sin^3\theta - 2\sqrt{2\epsilon}b_{,\chi}e^{-b}\sin^2\theta\cos\theta, \\ B &= -\eta_{,ss} + \eta_{,\sigma\sigma} - 2\epsilon + \sqrt{2\epsilon}b_{,\psi}\cos\theta(1+2\sin^2\theta) + \sqrt{2\epsilon}b_{,\chi}e^{-b}\sin\theta(2\sin^2\theta - 1) \\ &\quad + \frac{2}{3}\epsilon b_{,\psi}^2 + \frac{2}{3}\epsilon b_{,\psi\psi}, \end{aligned} \tag{3.10}$$

where $\eta_{,MN} = V_{,MN}/3H^2$ describes the curvature of the potential in terms of the entropy and adiabatic fields.

These functions encode the coupling between adiabatic and entropy modes and enter in the expressions for the spectral index and its runnings at the end of inflation that, in this general two-field model, can be derived from equation (2.12), equation (2.13), and equation (2.18) reading [196]

$$\begin{aligned} n_s &\simeq n_* - 2\sin\Theta(A_*\cos\Theta + B_*\sin\Theta), \\ \alpha_s &\simeq \alpha_* + 2\cos\Theta(A_*\cos\Theta + B_*\sin\Theta)\times(A_*\cos 2\Theta + B_*\sin 2\Theta), \\ \beta_s &\simeq \beta_* - 2\cos\Theta(A_*\cos\Theta + B_*\sin\Theta)\times(B_*\cos 2\Theta - A_*\sin 2\Theta) \\ &\quad \times(A_* + 2A_*\cos 2\Theta + B_*\sin 2\Theta). \end{aligned} \tag{3.11}$$

From the expressions above we see that constraints on the spectral parameters can be translated into constraints on the geometry of the field metric, namely the curved trajectory in field space between Hubble radius exit and the end of inflation.

3.2 Predictions

To be concrete and maintain control over the results, we test all the features of our method by analyzing a simple case where the coupling between the two fields is given by

$$b(\psi,\chi) = -c\,\frac{\psi\chi}{M_{\rm Pl}^2}, \tag{3.12}$$

with a self-coupling potential of the form

$$V = \frac{1}{2}m_\psi^2\psi^2 + \frac{1}{2}m_\chi^2\chi^2 + g^2\psi^2\chi^2, \tag{3.13}$$

where m_ψ and m_χ are the mass terms of the fields and g the coupling constant.

JCAP12(2023)014

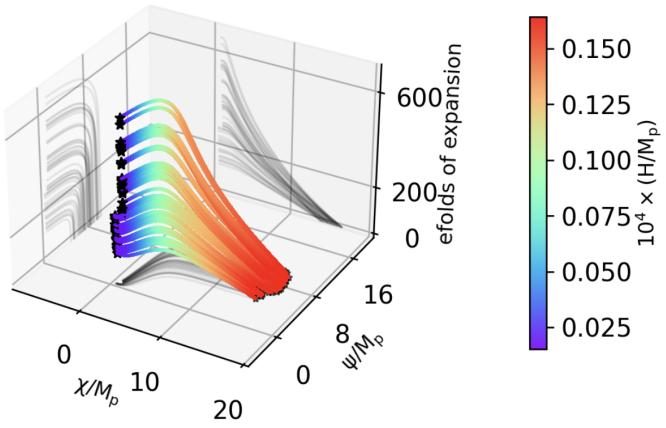

Figure 1. Field trajectories (as well as their projections in different 2D-planes in grey) as functions of the e-folds of expansions between the beginning of the integration and the end of inflation. The integration process begins at $N = 0$ with randomly selected initial conditions, represented by a black star-like dot in the figure. The end of inflation (marked by another black star-like dot) is determined using the method explained in subsection 2.2. The color-bar shows the value of the Hubble parameter along the field trajectories. For all trajectories, the model's free parameters are fixed to: $m_\psi = 1.58 \times 10^{-6}$, $m_\chi = 3.86 \times 10^{-6}$, $c = -0.06$, and $g = 2 \times 10^{-8}$.

Once the field metric and the self-coupling potential are specified, the formalism developed in the previous section can be applied and the multifield dynamics numerically solved by means of the integration scheme discussed in subsection 2.2. In particular, the integration of the equations of motion, and therefore the trajectory of the fields, will depend on the model's free parameters (i.e., m_ψ, m_χ, g and c) and the initial conditions of the fields (i.e., $\psi_{\rm ini}$, $\dot{\psi}_{\rm ini}$, $\chi_{\rm ini}$ and $\dot{\chi}_{\rm ini}$). In this subsection, we analyze separately the contribution of these parameters to both cosmological observables and the inflationary dynamics, in order to have a comprehensive understanding of their effect and to better interpret the results of the full Monte Carlo analysis performed in the subsequent subsection.

We start by examining the robustness of the outcomes of the model when subjected to variations in the initial conditions of the fields. Specifically, we evaluate how the trajectories in the field space change by randomly varying the starting points $\psi_{\rm ini}$ and $\chi_{\rm ini}$, while keeping the model's free parameters fixed and setting $\dot{\psi}_{\rm ini} = \dot{\chi}_{\rm ini} \simeq 0$. The results are depicted in figure 1. Considering different initial conditions for the fields can result in a period of inflation that is more or less long, while essentially keeping the model's predictions for cosmological observables unchanged. Therefore, we do not expect physical observables to drastically depend on the initial conditions of the fields.

On the other hand, the variation of the free parameters holds greater significance. For instance, the effects of c which are encoded in the curved field manifold play a substantial role in what concerns the interplay between isocurvature and curvature modes between the horizon crossing and the end of inflation. In particular, when c is gradually negatively reduced, the χ field velocity remains relatively constant and it becomes stuck for a significant amount of time until it reintegrates into the dynamics when the ψ field reaches the minimum of the potential, see also figure 2. This effect is translated into the amount of isocurvature mode feeding the curvature one. On the other hand, if c is progressively incremented will lead to a single field scenario as the χ field drops immediately.[8] In other words, the combination of curvature and

[8]Interestingly, models that exhibit this peculiar behavior, where a scalar field immediately drops and undergoes a phase of fast oscillations, have been the subject of study as they generate features in primordial

JCAP12(2023)014

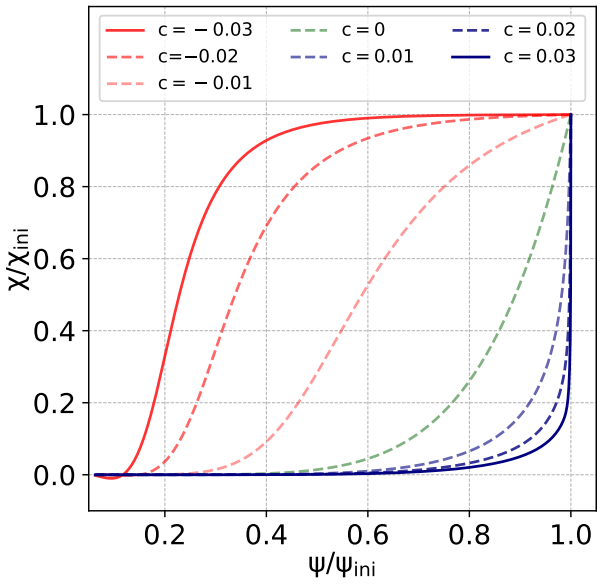

Figure 2. Effects of the field metric parameter c on the field evolution in the ψ vs χ plane. The field values have been normalized to their initial conditions, so the starting point of the trajectories is represented by the coordinates $(1, 1)$, while the coordinates $(0, 0)$ ideally represent the end of inflation. The red (blue) curves correspond to negative (positive) values of c as indicated in the legends, while the green curve corresponds to a flat filed metric $\mathcal{G}_{IJ} = \text{diag}\{1, 1\}$, (i.e., $c = 0$). The other model's free parameters are fixed to: $m_\psi = 1.58 \times 10^{-6}$, $m_\chi = 3.86 \times 10^{-6}$, and $g = 2 \times 10^{-8}$.

isocurvature perturbations may lack correlation. However, if the path in field space exhibits curvature from the Hubble exit until the end of inflation, it can introduce an indefinite level of correlation between them impacting the ultimate predictions and potentially causing their growth or reduction, see figure 3.

Shifting our focus to the effects of the masses, from figure 3 we can appreciate how changes in m_χ and m_ψ lead to increase or decrease of power in the spectrum of temperatures anisotropies. This can be explained by making explicit equation (2.8) as

$$V_{,\psi} \simeq -3\dot{\psi}H, \qquad V_{,\chi} \simeq -3\dot{\chi}e^{2b(\psi,\chi)}H, \tag{3.14}$$

and taking into account a self-coupling potential of the form equation (3.13), one can easily get

$$V_{,\chi\chi} = 2b_{,\chi}V_{,\chi} - 3e^{2b(\psi,\chi)}\dot{H}, \tag{3.15}$$

by means of $\frac{dH}{d\chi} = \frac{\dot{H}}{\dot{\chi}}$. Finally, we achieve the following relation

$$m_\chi^2 = 2b_{,\chi}V_{,\chi} + \frac{3}{2}\dot{\sigma}^2 e^{2b(\psi,\chi)} - 2g^2\psi^2. \tag{3.16}$$

Therefore, on the slow-roll trajectory defined by equation (3.15) there is a correlation between the mass m_χ and the coupling $b_{,\chi}$. Such a correlation does not exist for m_ψ, for which we obtain

$$m_\psi^2 = \frac{3}{2}\dot{\sigma}^2 - 2g^2\chi^2, \tag{3.17}$$

density perturbations that directly record the scale factor evolution $a(t)$ while serving as "standard clocks" in the primordial Universe, see e.g., refs. [197–200].

JCAP12(2023)014

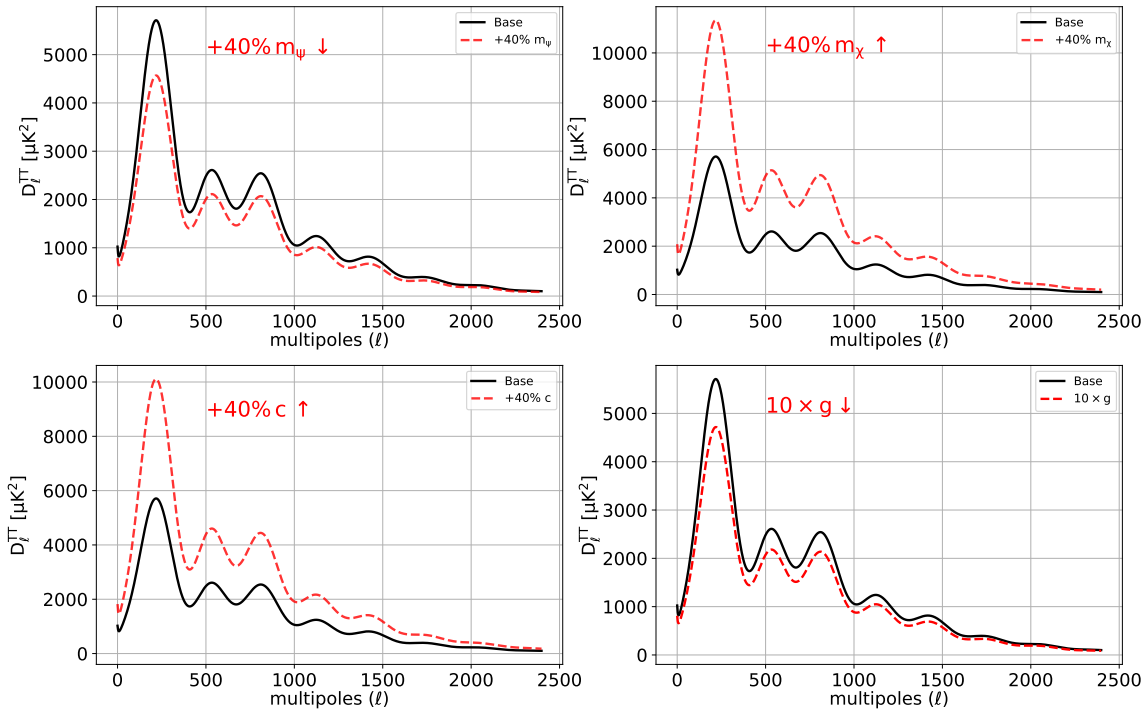

Figure 3. Effects on the CMB angular power spectrum resulting from variations in the model's parameters as indicated in the different panels/legends of the figure. The baseline model (black line) corresponds to the following parameter combination: $m_\psi = 1.58\times10^{-6}$, $m_\chi = 3.86\times10^{-6}$, $c = -0.06$, and $g = 2\times10^{-8}$.

stating that an increase in m_ψ leads to a rapid change in the Hubble rate ($\dot{\sigma}^2 \simeq -\dot{H}$) which translates into a shorter period of inflation and hence a reduction of the amplitude of the power spectrum as seen in figure 3. The same figure shows that increasing either c and m_χ results in a larger amplitude of the initial power spectrum, as expected from equation (3.16).

3.3 Monte Carlo analysis and parameter constraints

We use the sampling algorithm detailed in subsection 2.3 to explore the parameter space of our multifield model. The sampling involves 4 free parameters (m_ψ, m_χ, g, and c) and the initial conditions of the fields ($\psi_{\rm ini}$, $\chi_{\rm ini}$), which determine the field trajectory during inflation, as pointed out in subsection 3.2. To ensure that we are able to explore a sufficiently large volume of the parameter space, we randomly vary the model parameters and initial conditions in the large uniform priors listed in table 1. This enables us to obtain a number of combinations of parameters and initial conditions as large as the number of steps in the Monte Carlo analysis. For each step, we use the integration algorithm described in subsection 2.2 and compute the full evolution of the fields as well as any observable quantities of the model, including all the primordial scalar and tensor spectrum parameters such as A_s, n_s, α_s, β_s and r. We test the agreement of each combination of parameter and initial conditions against data by using our likelihood equation (2.19) built on the Planck-2018 [191–194] and BK18 [9] observations of the cosmic microwave background temperature and polarization anisotropies.

Following this methodology, we perform a full Monte Carlo analysis, repeating the process for $\gtrsim 5\times10^6$ steps and collecting about 2×10^4 sampled models, each of one with

JCAP12(2023)014

Initial Conditions	Constraints	Unifrom Prior Ranges
$\psi_{\rm ini}/M_p$	–	$\psi_{\rm ini}/M_p \in [14\,,\,17]$
$\chi_{\rm ini}/M_p$	–	$\chi_{\rm ini}/M_p \in [10\,,\,4]$
Model's Parameters	Constraints	Unifrom Prior Ranges
m_ψ	$< 2.30 \cdot 10^{-6}$	$\log_{10}(m_\psi) \in [-8\,,\,-4]$
m_χ	$< 1.01 \cdot 10^{-5}$	$\log_{10}(m_\chi) \in [-8\,,\,-4]$
c	< -0.0211	$c \in [-1\,,\,1]$
g	$< 9.72 \cdot 10^{-7}$	$\log_{10}(g) \in [-8\,,\,-5]$
Primordial spectra	Constraints	
A_s	$(\,2.109 \pm 0.033\,) \cdot 10^{-9}$	
n_s	$0.9621^{+0.0053}_{-0.0047}$	
α_s	$\left(-0.74^{+0.37}_{-0.32}\right) \times 10^{-3}$	
β_s	$\left(-0.103^{+0.088}_{-0.0040}\right) \times 10^{-3}$	
r	< 0.04	
Entropy Transfer	Constraints	
Θ	< -0.686	
$A_\star$	> -1.71	
$B_\star$	> -0.341	

Table 1. External priors and observational constraints at 1σ (68% C.L.) or upper bounds are at 2σ (95% C.L.) on parameters.

its own likelihood. In this way, we derive informative posterior distributions for all the parameters involved in the sampling, as well as for any derived quantities of interest, including those associated with entropy transfer on super-horizon scales. The results are summarized in table 1, while figure 4 depicts the distribution of the sampled models in the 4D parameter space, represented by a box with dimensions corresponding to the size of the prior volume. Figure 5 shows instead the 68% and 95% CL contour plots for all the quantities of interest in the model.

The first important test we can perform is to study the constraints on the inflationary observables, such as the amplitude of the primordial scalar spectrum A_s, the spectral index n_s, its runnings α_s and β_s, and the amplitude of primordial tensor modes r. Notice that when dealing with multifield inflation, fixing a model does not necessarily establish consistency relations between these parameters as it usually happens in single-field inflation. Consequently, the specific values of these observables depend on the interplay between the free parameters of the model and the initial conditions of the fields. Additionally, it is important to account for corrections that arise due to the super-horizon evolution of adiabatic and isocurvature perturbations, as discussed in previous sections. Regarding the amplitude of the scalar spectrum, we obtain $A_s = (\,2.109 \pm 0.033\,) \cdot 10^{-9}$ at 68% CL, in perfect agreement with the model-independent analysis performed with the full Planck and BK18 likelihoods (see also appendix B). Similarly, for the spectral index we get $n_s = 0.9621^{+0.0053}_{-0.0047}$ at 68%

JCAP12(2023)014

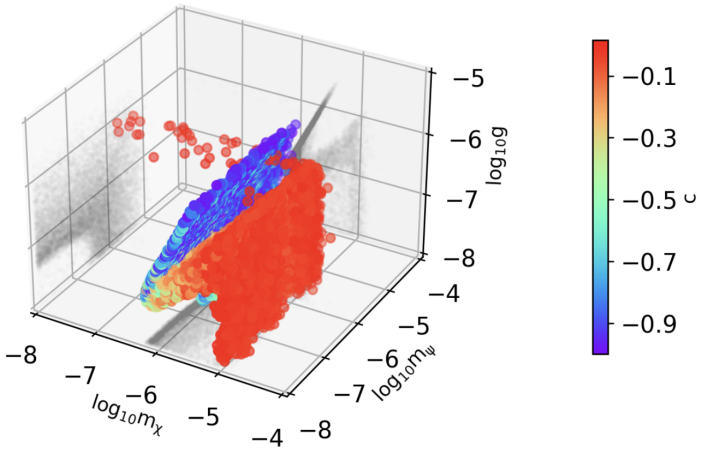

Figure 4. How the models distribute in the 4-dimensional parameter space. The box has the size of the prior volume.

CL, while the for the amplitude of primordial gravitational waves we obtain an upped bound $r < 0.04$ at 95% CL. All these results are consistent with the most recent joint analyses of Planck and BK18 data, as well. Regarding the higher-order runnings of the primordial scalar spectrum, we obtain at 68 % CL $\alpha_s = \left(-0.74^{+0.37}_{-0.32}\right) \times 10^{-3}$ and $\beta_s = \left(-0.103^{+0.088}_{-0.004}\right) \times 10^{-3}$, respectively. Therefore, assuming this particular multifield model, smaller negative values are favored for both the running and the running of the running, although both of them remain consistent with null values at 95% CL.

One significant aspect of our approach is the ability to obtain observational constraints on the model parameters. For instance, within this particular model, we are able to place a 95% CL upper bound on the mass values of the fields that (in Planck units) read $m_\psi < 2.30 \cdot 10^{-6}$ and $m_\chi < 1.01 \cdot 10^{-5}$, respectively. Similarly, for the coupling parameter g we obtain $g < 9.72 \cdot 10^{-7}$ at 95% CL, while for the parameter c controlling the curvature of the filed space we obtain $c < -0.0211$ always at 95% CL. It is worth noting that these upper bounds assume values significantly far from the limits of the priors adopted for these parameters. In this regard, we have verified that the priors chosen for parameter exploration are sufficiently large to provide uninformative ranges, without introducing any unwanted bias in the parameter constraints. In order to study the correlation between the different parameters, we can refer to figure 3 for the effects on the angular spectra, figure 4 for the correlation in the 4-D parameter space of the model, and figure 5 for the contour plot with all sampled and derived parameters. From figure 3, one would expect a correlation between the effects of the parameters g and c on the spectrum of CMB temperature anisotropies as considering more negative values of c leads to a power amplification, while increasing g reduces the amplitude of the spectrum. Therefore, we expect that more negative values of c can be allowed only for larger values of g, and this is clearly confirmed by both figure 4 and figure 5. Notice also that this model strongly prefers highly negative values of c. The reason behind this preference is that when c becomes positive, the curvature of the field space $\mathcal{G}_{IJ}(\phi^K)$ is exponentially suppressed, and one of the two fields essentially becomes a spectator field. As a result, the model reduces to a single-field model with a quadratic potential, which is well-known to predict a significantly large amount of primordial gravitational waves, higher than the current observational limit. Therefore, the parameter space with positive values of

JCAP12(2023)014

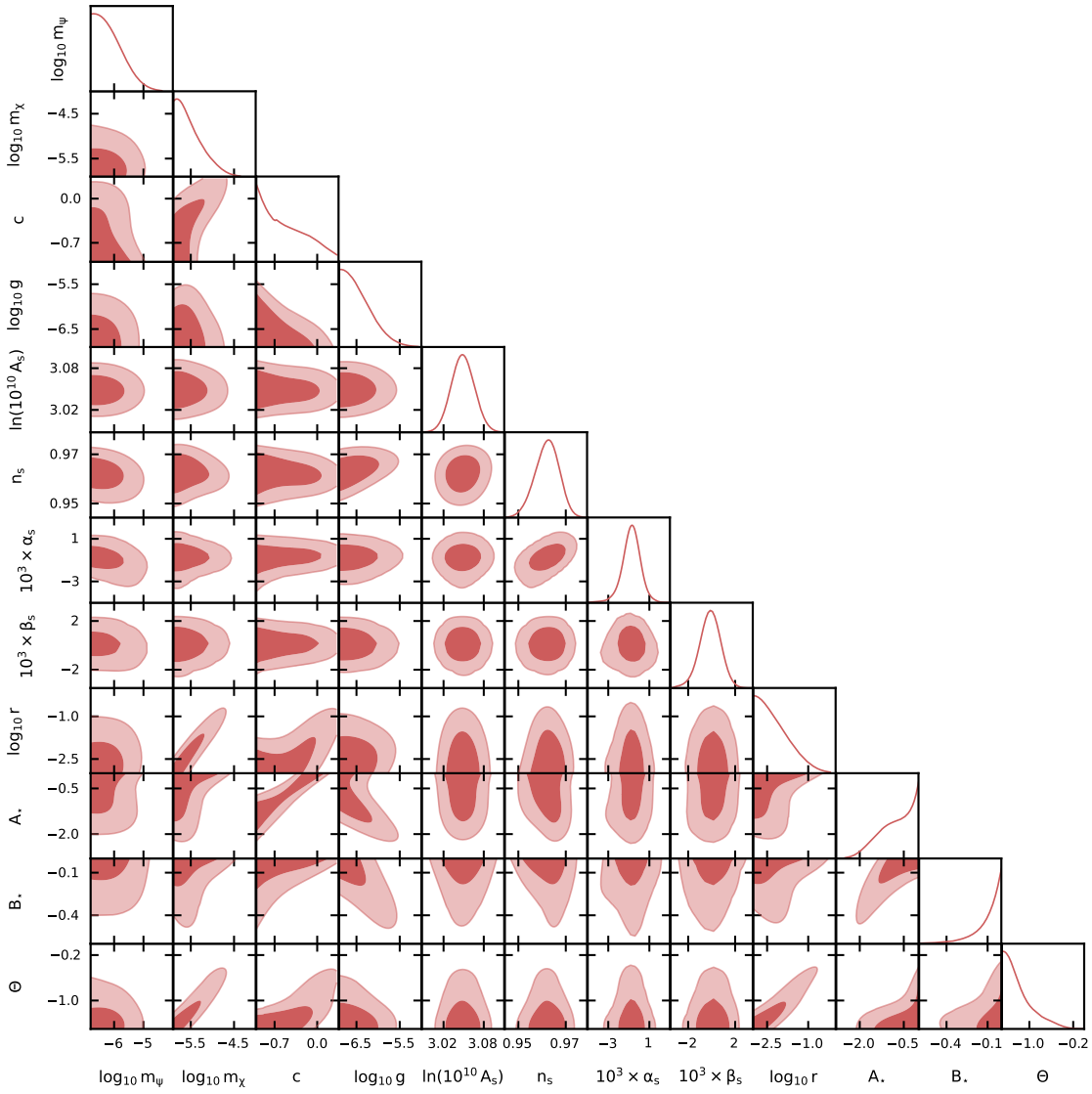

Figure 5. Marginalized 2D and 1D posteriors distributions for all the model's parameters and the quantities of interests in this study.

c is severely constrained by the B-mode polarization measurements by BK18, in combination with the Planck temperature and polarization measurements.

Finally, our algorithm allows us to derive constraints on any relevant physical quantities in the model, including parameters and functions that govern the transfer of entropy between adiabatic and isocurvature perturbations. For example, we derive a 95% CL upper bound on the angle $\Theta < -0.686$ appearing in equation (3.11) that weights the corrections acquired by the inflationary parameters between the Hubble exit and the end of inflation. Similarly, we can constrain the time-dependent functions $A(t)$ and $B(t)$ involved in the transfer matrix formalism used to account for the correlation between curvature and isocurvature modes, as well as to estimate the transfer of entropy from the latter to the former during the time from soon after the Hubble exit to the end of inflation. We evaluate these functions at the

JCAP12(2023)014

Hubble exit, finding at 95%CL the following limits $A_\star > -1.71$ and $B_\star > -0.341$. Our results confirm that in multi-field models with non-flat field metric, the interplay between isocurvature and adiabatic modes plays a crucial role in the final observable predictions, as already argued in ref. [124].

4 Conclusion

Embedding inflation within a more fundamental framework still remains an open problem, and numerous models and mechanisms have been proposed. The simplest dynamical models of inflation involve a single scalar field minimally coupled to gravity whose evolution is governed by a potential that should be enough flat to induce a phase of slow-roll evolution. However, in certain low-energy effective field theories inspired by string theory, the scalar field sector often comprises multiple scalar fields with non-standard kinetic terms or dynamical couplings. When inflation is driven by multiple scalar fields with non-standard kinetic terms, the interplay between adiabatic perturbations and isocurvature modes becomes significant, influencing the observable predictions and giving rise to a rich phenomenology that can be tested using current cosmological and astrophysical data. In principle, precise measurements of the cosmic microwave background radiation can be used, providing stringent constraints on the abundance of both adiabatic and isocurvature modes and offering a valuable opportunity for experimental validation of these models/theories. However, in practice, obtaining precise predictions from multifield inflation is not always easy as observational quantities often depend on various factors such as the initial conditions of the fields and the specific model assumed. Different trajectories in field space can lead to different results, changing the amplitude of scalar and tensor primordial perturbations. For this reason, most tools employed in cosmological data analyses, such as typical Boltzmann integrator codes and samplers, are either unaware of the physics of inflation or assume single-field potentials. As a result, constraining the multifield landscape with current CMB data represents an ongoing challenge.

In this work, we take a first step to bridge this gap and introduce an algorithm specifically designed to investigate generic multifield models of inflation where a number of scalar fields ϕ^K are minimally coupled to gravity and live in a field space with a non-trivial metric $\mathcal{G}_{IJ}(\phi^K)$. In section 2, we describe both our theoretical parameterization and our numerical method. In particular, after specifying the initial conditions for the fields ϕ^K, their velocities, the metric $\mathcal{G}_{IJ}(\phi^K)$ of the field space, and the self-coupling potential, our algorithm is able to reconstruct the dynamics of the fields throughout the entire inflationary period precisely determining the end of inflation and performing several consistency tests to ensure the stability of the model. This comprehensive analysis includes more intricate scenarios where distinct field dynamics govern various stages of expansion at different times, such as double inflation or punctuated inflation. An illustrative example can be found in appendix A. By numerically solving the full field dynamics, we can calculate precise predictions for observable quantities in the slow-roll limit, such as the spectrum of scalar perturbations, primordial gravitational waves, and isocurvature modes. We can also track the super-horizon dynamics of adiabatic and isocurvature modes, determining the transfer of entropy to scalar modes after horizon crossing using the transfer matrix formalism described in subsection 2.1. Once the integration process successfully concludes, we can access all the observable predictions of the model and set the initial conditions to compute the subsequent cosmology. This is done by interfacing our algorithm with standard Boltzmann integrator codes such as `CAMB` or `CLASS` that allow

JCAP12(2023)014

us to directly translate the model's predictions in terms of the cosmic microwave background anisotropies and polarization angular power spectra.

Based on this algorithm, we also introduce a novel sampler which is specifically designed to explore a sufficiently large volume of the parameter space of a generic multifield models and identify a sub-region where the model's predictions are in agreement with observations. This allows us to efficiently sample over the initial conditions of the fields and the free parameters of the model, enabling Monte Carlo analysis to compare theoretical predictions with observations. In this work, we make use of the most recent CMB data provided by the Planck collaboration, as well as the latest B-modes power spectrum likelihood released by the Bicep/Keck Array X Collaboration and extract a likelihood for each sampled combinations of parameters. To do so, we develop an analytical likelihood based on these observations that has been extensively tested and proven to reproduce the results obtained from the real likelihoods of different experiments for inflationary parameters, see appendix B.

In section 3, we provide a detailed illustration of our approach by analyzing a specific case study model where two scalar fields are coupled through the field metric by equation (3.12), with a self-coupling potential given by equation (3.13). Focusing on this model, in subsection 3.2 we use our integration scheme to investigate how the observable predictions change with its parameters and initial conditions. We refer to figure 1 and figure 2 for the impact of the field trajectories and the coupling function, respectively. Instead figure 3 illustrates the impact of the different parameters on the CMB angular power spectra of temperature anisotropies. Finally, in subsection 3.3, we employ our sampler to perform a comprehensive Monte Carlo analysis, deriving observational constraints on the free parameters. The results of our analysis are summarized in table 1, while figure 4 and figure 5 show the distribution of sampled models in the parameter space and the correlation among the different parameters, respectively. We are able to derive compelling and precise constraints on both the model's parameters and the inflationary observables such as the primordial power spectra of scalar and tensor perturbations. In addition, we can place constraints on the interplay between curvature and isocurvature modes by accurately accounting for the entropy transfer from isocurvature to curvature perturbations on superhorizon scales. For sake of completeness, in appendix A, we also discuss the limit where the model reduces to the case of a double quadratic potential with a canonical kinetic term, discussing our ability to recover results already documented in the literature.

Our work provides a robust framework for exploring multifield inflation and opens up exciting opportunities for future research focused on the rich phenomenology expected in both standard and non-standard multifield models of inflation and gravity.

Acknowledgments

CvdB is supported (in part) by the Lancaster-Manchester-Sheffield Consortium for Fundamental Physics under STFC grant: ST/T001038/1. EDV is supported by a Royal Society Dorothy Hodgkin Research Fellowship. This article is based upon work from COST Action CA21136 Addressing observational tensions in cosmology with systematics and fundamental physics (CosmoVerse) supported by COST (European Cooperation in Science and Technology). We acknowledge IT Services at The University of Sheffield for the provision of services for High Performance Computing.

JCAP12(2023)014

A Double quadratic potential & double inflation

In this appendix, we make use of our code to briefly examine a simplified two-field model compared to the one analyzed in section 3. Specifically, we investigate the case of a double-field quadratic potential with a canonical kinetic term

$$V = \frac{1}{2}m_\psi^2\psi^2 + \frac{1}{2}m_\chi^2\chi^2 \tag{A.1}$$

which falls within the parameterization adopted in section 3 once we fix $c = 0$ and $g = 0$.

Notice that this model has been already discussed in the literature and a comprehensive systematic review of its properties is beyond the goal of our work. That being said, this appendix serves a dual purpose: on one side, we aim to use this simplified case as a safety check to demonstrate our ability to recover many of the results already documented in the literature. On the other hand, we take this opportunity to provide a working example of some features of our algorithm, such as its ability to correctly identify the end of inflation and effectively handle scenarios of double inflation where two stages of expansions are driven by distinct fields at distinct times.[9]

Regarding the topic of interest for our discussion, an analysis similar to the one we carry on here is given in ref. [201] where, using a parameterization for the inflationary dynamics very close to the one we have developed in this paper, the authors point out the characteristics of this two-field model, deriving predictions for observables such as the amplitude of primordial spectra. As highlighted in section III.C of ref. [201], a distinctive feature of this potential is the prediction of a tensor-to-scalar-ratio $r \gtrsim 0.13$, regardless of the initial conditions for the fields and the values of the mass ratio. Given that a similar value for the tensor amplitude does not appear to be in agreement with the most recent measurements of CMB B-mode polarization released by the Keck Array collaboration, we do not perform a data analysis (which would be inconclusive given the model's inability to reconcile with the latest observations). However, we perform a model sampling as a cross-validation of the predictions for r. As seen in figure 6, collecting approximately 10^4 models where the amplitude of the scalar spectrum A_s and its tilt n_s fall within ranges consistent with our observational data, we find that the tensor amplitude r remains consistently above the 95% limit resulting from the joint Planck+BK18 analysis. Furthermore, the value of r predicted by this potential remains largely unchanged both with respect to the mass ratio (across multiple orders of magnitude) and with respect to the initial conditions (which are randomly chosen from model to model) as well as in excellent agreement with figure 8 of ref. [201].

A closer analysis of the figure reveals the presence of a minor dispersion of patterns that deviate from the degeneration line between the mass ratio and the value of r. A detailed analysis of these models has revealed that this small dispersion is due to double inflation. While theoretically investigated, in ref. [201] these models were not given thorough consideration and the inflationary dynamics were computed by treating double inflation as if it consists of only one inflationary phase. However, as explained in subsection 2.2, our algorithm has been designed to accurately identify all inflationary phases and comprehensively reconstruct their dynamics. As a result, we can provide precise predictions for scenarios involving double inflation, as well.

[9] It is worth noting that these scenarios are more commonly realized in models of double quadratic potential with canonical kinetic terms than in the models detailed in section 3.

JCAP12(2023)014

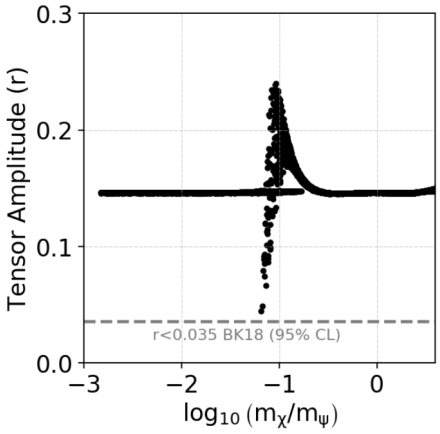

Figure 6. Predictions for the tensor amplitude r in terms of the mass ratio $\log_{10}(m_\chi/m_\psi)$ for $\sim 10^4$ models where the amplitude of the scalar spectrum A_s and its tilt n_s fall within ranges consistent with our observational data.

To put it more quantitatively and clarify our treatment of double inflation, we focus on one specific model among those depicted in figure 6. Namely, we consider the one which shows the smallest tensor amplitude ($r \sim 0.05$, yet outside the Planck-BK18 range) and provide full details of the dynamics of the field and the background evolution in figure 7. As evident from the top panel of the figure, in this model, the parameter ϵ reaches the critical value $\epsilon = 1$ for the first time after about 55 e-folds (grey dashed line). During this initial phase, the expansion of the Universe is driven by the field ψ, whose evolution is depicted in the second panel of the same figure. As one can observe, when $\epsilon = 1$, the dynamics of ψ is mostly completed, while the second field χ (whose evolution is shown in the third panel) remains mostly inactive during this phase. Once the inflationary stage guided by ψ terminates, our algorithm monitors the dynamics of the fields and, since χ is still very active, the integration of the equation of motion continues until the second field also completes its dynamics. This allows us to identify a second inflationary phase, this time guided by χ. In both of these stages, the background dynamics, represented by the evolution of the Hubble parameter H (bottom panel), is accurately computed together with all observational predictions, including the tensor amplitude.

B Sampling and likelihood validation

In this appendix, we provide a step by step explanation of the methodology used to build our likelihood based on the joint analysis of B-Modes polarization data from BK18 and the Planck-2018 measurements of temperature and polarization anisotropies. Most importantly, we prove that our method/likelihood is able to reproduce the same results obtained by the most commonly Markov Chain Monte Carlo (MCMC) analyses performed in the literature. To do this, through all this appendix, we do not consider any explicit inflationary models, and remain completely agnostic about the physics of inflation, as customary in the literature.

1) As a first step, we consider an extension to the standard cosmological model which includes three additional parameters: the tensor amplitude r, the running of the spectral index α_s, and the running of the running β_s. We refer to this model as

JCAP12(2023)014

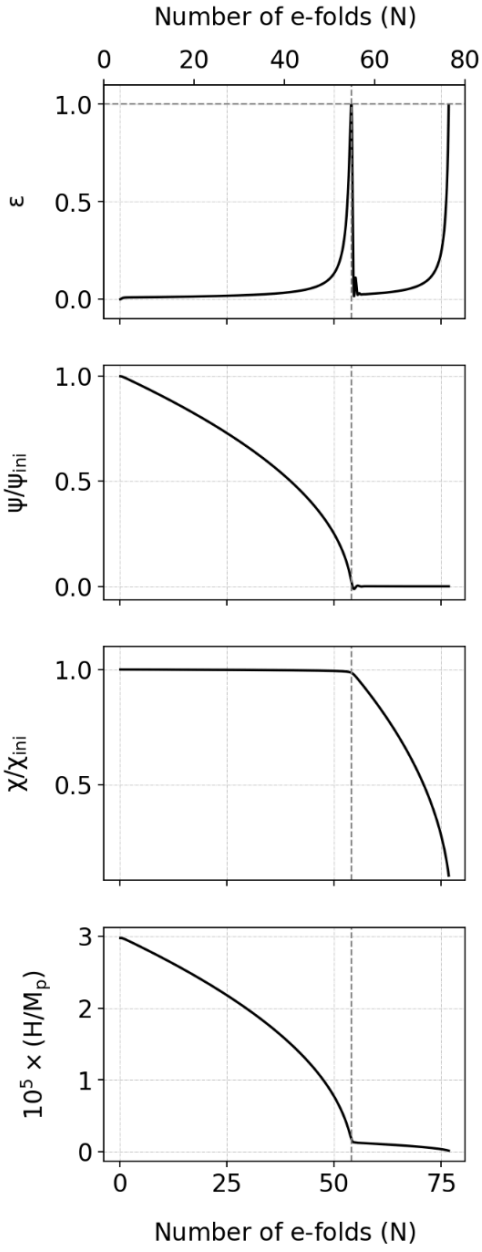

Figure 7. Evolution of the parameter ϵ (top panel), the scalar fields ψ and χ (second and third panel, respectively), and the Hubble parameter H (bottom panel) in a model of double inflation characterized by two stages of expansion.

JCAP12(2023)014

ΛCDM+α_s+β_s+r and perform a full Monte Carlo Markov Chain (MCMC) analysis using the publicly available sampler `Cobaya` [202], and Boltzmann integrator code `CAMB` [173, 174]. `Cobaya` explores the posterior distributions of the parameter space using the MCMC sampler developed for `CosmoMC`[203], which has been specifically adapted for parameter spaces with a hierarchy of speeds by implementing the "fast dragging" procedure introduced in ref. [204]. The baseline datasets involved in our MCMC analysis consist of the Planck 2018 temperature and polarization (TT TE EE)

Parameter	Real likelihoods	This work
$\log(10^{10}A_{\rm S})$	3.049 ± 0.016	3.051 ± 0.015
$n_{\rm s}$	0.9624 ± 0.0044	0.9621 ± 0.0046
$\alpha_{\rm s}$	0.002 ± 0.010	0.002 ± 0.010
$\beta_{\rm s}$	0.012 ± 0.012	0.013 ± 0.013
r	< 0.0354	< 0.0357

Table 2. Results for the ΛCDM+α_s+β_s+r model obtained using the publicly available sampler `Cobaya` [202] in combination with the full Planck 2018 [191–194] and BK18 [9] likelihoods (referred to as 'Real likelihoods'), and the results for the same model derived using our sampling algorithm in combination with our analytical likelihood (equation (2.19)) (referred to as 'This work').

likelihood, which includes low multipole data ($\ell < 30$) [191–193], as well as the lensing likelihood obtained from measurements of the power spectrum of the lensing potential [194]. Additionally, we include the most recent CMB B-modes power spectrum likelihood cleaned from foreground contamination, as released by the Bicep/Keck Array X Collaboration [9]. The resulting constraints are presented in table 2, and we also take this opportunity to update the current bounds on this cosmological extension with the latest data.

2) As a second step, using the results from our MCMC analyses, we construct our analytical likelihood based on equation (2.19). In particular, we adopt the generalized covariance matrix Σ and the mean values μ of parameters obtained for the ΛCDM+α_s+β_s+r model.

3) Finally, we test that our likelihood is able to reproduce the same constraints as real likelihoods from experiments. This is a crucial step needed to validate the results obtained when our likelihood is applied to the study of physical models of multifield inflation. To prove the equivalence of our method and the MCMC analysis, we perform a consistency check for the same ΛCDM+α_s+β_s+r cosmological model. Specifically, we perform a new run varying the inflationary parameters $\{A_s,\, n_s,\, \alpha_s,\, \beta_s\}$ using our sampling algorithm. In this case, the sampling is performed directly in the parameter space of inflationary observables and using the same prior ranges used for the MCMC analyses. Since sampling on the inflationary parameters requires significantly fewer computational resources, avoiding also some non-physical behaviors that may arise when exploring non-standard inflationary models or solving the inflationary dynamics, we are able to accumulate $\sim 10^5$ models, each of them evaluated using our analytical likelihood equation (2.19). In figure 8, we directly compare the results obtained using our approach (labeled as 'this work') to the results obtained using the real likelihoods from experiments and the sampler `Cobaya` (labeled as 'Real likelihoods'). The two methods yield the same constraints for all inflationary parameters, see also table 2.

JCAP12(2023)014

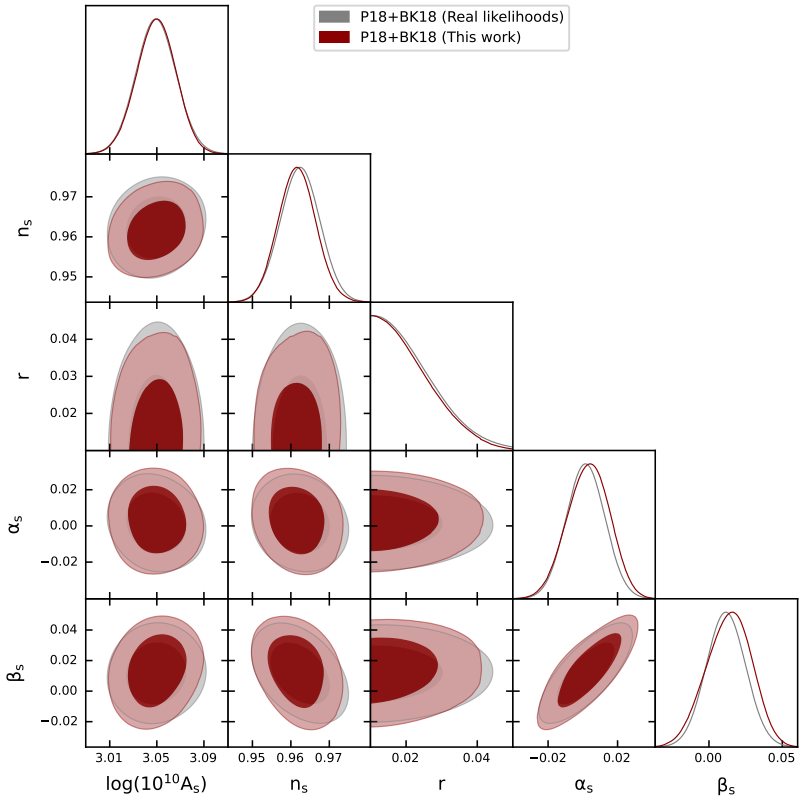

Figure 8. Marginalized 2D and 1D posteriors distributions for the ΛCDM+α_s+β_s+r model obtained using the publicly available sampler `Cobaya` [202] in combination with the full Planck 2018 [191–194] and BK18 [9] likelihoods (grey), and our sampling algorithm in combination with our analytical likelihood (red).

References

[1] A.H. Guth, *The Inflationary Universe: A Possible Solution to the Horizon and Flatness Problems*, *Phys. Rev. D* **23** (1981) 347 [INSPIRE].

[2] A.D. Linde, *A New Inflationary Universe Scenario: A Possible Solution of the Horizon, Flatness, Homogeneity, Isotropy and Primordial Monopole Problems*, *Phys. Lett. B* **108** (1982) 389 [INSPIRE].

[3] A. Albrecht and P.J. Steinhardt, *Cosmology for Grand Unified Theories with Radiatively Induced Symmetry Breaking*, *Phys. Rev. Lett.* **48** (1982) 1220 [INSPIRE].

[4] V.F. Mukhanov and G.V. Chibisov, *Quantum Fluctuations and a Nonsingular Universe*, *JETP Lett.* **33** (1981) 532 [INSPIRE].

[5] J.M. Bardeen, P.J. Steinhardt and M.S. Turner, *Spontaneous Creation of Almost Scale-Free Density Perturbations in an Inflationary Universe*, *Phys. Rev. D* **28** (1983) 679 [INSPIRE].

[6] S.W. Hawking, *The Development of Irregularities in a Single Bubble Inflationary Universe*, *Phys. Lett. B* **115** (1982) 295 [INSPIRE].

[7] A.H. Guth and S.Y. Pi, *Fluctuations in the New Inflationary Universe*, *Phys. Rev. Lett.* **49** (1982) 1110 [INSPIRE].

[8] Planck collaboration, *Planck 2018 results. X. Constraints on inflation*, *Astron. Astrophys.* **641** (2020) A10 [arXiv:1807.06211] [INSPIRE].

JCAP12(2023)014

[9] BICEP and Keck collaborations, *Improved Constraints on Primordial Gravitational Waves using Planck, WMAP, and BICEP/Keck Observations through the 2018 Observing Season*, *Phys. Rev. Lett.* **127** (2021) 151301 [arXiv:2110.00483] [INSPIRE].

[10] W. Lin and M. Ishak, *A Bayesian interpretation of inconsistency measures in cosmology*, *JCAP* **05** (2021) 009 [arXiv:1909.10991] [INSPIRE].

[11] M. Forconi, W. Giarè, E. Di Valentino and A. Melchiorri, *Cosmological constraints on slow roll inflation: An update*, *Phys. Rev. D* **104** (2021) 103528 [arXiv:2110.01695] [INSPIRE].

[12] W. Handley and P. Lemos, *Quantifying the global parameter tensions between ACT, SPT and Planck*, *Phys. Rev. D* **103** (2021) 063529 [arXiv:2007.08496] [INSPIRE].

[13] A. La Posta, U. Natale, E. Calabrese, X. Garrido and T. Louis, *Assessing the consistency between CMB temperature and polarization measurements with application to Planck, ACT, and SPT data*, *Phys. Rev. D* **107** (2023) 023510 [arXiv:2204.01885] [INSPIRE].

[14] E. Di Valentino, W. Giarè, A. Melchiorri and J. Silk, *Quantifying the global 'CMB tension' between the Atacama Cosmology Telescope and the Planck satellite in extended models of cosmology*, *Mon. Not. Roy. Astron. Soc.* **520** (2023) 210 [arXiv:2209.14054] [INSPIRE].

[15] E. Di Valentino, W. Giarè, A. Melchiorri and J. Silk, *Health checkup test of the standard cosmological model in view of recent cosmic microwave background anisotropies experiments*, *Phys. Rev. D* **106** (2022) 103506 [arXiv:2209.12872] [INSPIRE].

[16] W. Giarè, F. Renzi, O. Mena, E. Di Valentino and A. Melchiorri, *Is the Harrison-Zel'dovich spectrum coming back? ACT preference for $n_s \sim 1$ and its discordance with Planck*, *Mon. Not. Roy. Astron. Soc.* **521** (2023) 2911 [arXiv:2210.09018] [INSPIRE].

[17] R. Calderón, A. Shafieloo, D.K. Hazra and W. Sohn, *On the consistency of ΛCDM with CMB measurements in light of the latest Planck, ACT and SPT data*, *JCAP* **08** (2023) 059 [arXiv:2302.14300] [INSPIRE].

[18] W. Giarè, *CMB Anomalies and the Hubble Tension*, arXiv:2305.16919 [INSPIRE].

[19] W. Giarè, S. Pan, E. Di Valentino, W. Yang, J. de Haro and A. Melchiorri, *Inflationary Potential as seen from Different Angles: Model Compatibility from Multiple CMB Missions*, *JCAP* **09** (2023) 019 [arXiv:2305.15378] [INSPIRE].

[20] A.G. Riess et al., *A Comprehensive Measurement of the Local Value of the Hubble Constant with 1 km s^{-1} Mpc^{-1} Uncertainty from the Hubble Space Telescope and the SH0ES Team*, *Astrophys. J. Lett.* **934** (2022) L7 [arXiv:2112.04510] [INSPIRE].

[21] L. Verde, T. Treu and A.G. Riess, *Tensions between the Early and the Late Universe*, *Nature Astron.* **3** (2019) 891 [arXiv:1907.10625] [INSPIRE].

[22] E. Di Valentino et al., *Snowmass2021 — Letter of interest cosmology intertwined II: The hubble constant tension*, *Astropart. Phys.* **131** (2021) 102605 [arXiv:2008.11284] [INSPIRE].

[23] E. Di Valentino et al., *In the realm of the Hubble tension—a review of solutions*, *Class. Quant. Grav.* **38** (2021) 153001 [arXiv:2103.01183] [INSPIRE].

[24] E. Abdalla et al., *Cosmology intertwined: A review of the particle physics, astrophysics, and cosmology associated with the cosmological tensions and anomalies*, *JHEAp* **34** (2022) 49 [arXiv:2203.06142] [INSPIRE].

[25] E. Di Valentino, A. Melchiorri, Y. Fantaye and A. Heavens, *Bayesian evidence against the Harrison-Zel'dovich spectrum in tensions with cosmological data sets*, *Phys. Rev. D* **98** (2018) 063508 [arXiv:1808.09201] [INSPIRE].

[26] G. Ye, J.-Q. Jiang and Y.-S. Piao, *Toward inflation with $n_s = 1$ in light of the Hubble tension and implications for primordial gravitational waves*, *Phys. Rev. D* **106** (2022) 103528 [arXiv:2205.02478] [INSPIRE].

JCAP12(2023)014

[27] J.-Q. Jiang and Y.-S. Piao, *Toward early dark energy and ns=1 with Planck, ACT, and SPT observations*, *Phys. Rev. D* **105** (2022) 103514 [arXiv:2202.13379] [INSPIRE].

[28] J.-Q. Jiang, G. Ye and Y.-S. Piao, *Return of Harrison-Zeldovich spectrum in light of recent cosmological tensions*, arXiv:2210.06125 [INSPIRE].

[29] F. Takahashi and W. Yin, *Cosmological implications of $n_s \approx 1$ in light of the Hubble tension*, *Phys. Lett. B* **830** (2022) 137143 [arXiv:2112.06710] [INSPIRE].

[30] C.-M. Lin, *D-term inflation in braneworld models: Consistency with cosmic-string bounds and early-time Hubble tension resolving models*, *Phys. Rev. D* **106** (2022) 103511 [arXiv:2204.10475] [INSPIRE].

[31] D.K. Hazra, A. Antony and A. Shafieloo, *One spectrum to cure them all: signature from early Universe solves major anomalies and tensions in cosmology*, *JCAP* **08** (2022) 063 [arXiv:2201.12000] [INSPIRE].

[32] M. Braglia, X. Chen and D.K. Hazra, *Uncovering the history of cosmic inflation from anomalies in cosmic microwave background spectra*, *Eur. Phys. J. C* **82** (2022) 498 [arXiv:2106.07546] [INSPIRE].

[33] R.E. Keeley, A. Shafieloo, D.K. Hazra and T. Souradeep, *Inflation Wars: A New Hope*, *JCAP* **09** (2020) 055 [arXiv:2006.12710] [INSPIRE].

[34] J.-Q. Jiang, G. Ye and Y.-S. Piao, *Impact of the Hubble tension on the r-n_s contour*, arXiv:2303.12345 [INSPIRE].

[35] J. Martin, C. Ringeval, R. Trotta and V. Vennin, *The Best Inflationary Models After Planck*, *JCAP* **03** (2014) 039 [arXiv:1312.3529] [INSPIRE].

[36] D.H. Lyth and A. Riotto, *Particle physics models of inflation and the cosmological density perturbation*, *Phys. Rept.* **314** (1999) 1 [hep-ph/9807278] [INSPIRE].

[37] A.D. Linde, *Inflationary Cosmology*, *Lect. Notes Phys.* **738** (2008) 1.

[38] D. Baumann and L. McAllister, *Inflation and String Theory*, *Cambridge Monographs on Mathematical Physics*, Cambridge University Press (2015).

[39] S.M. Leach, A.R. Liddle, J. Martin and D.J. Schwarz, *Cosmological parameter estimation and the inflationary cosmology*, *Phys. Rev. D* **66** (2002) 023515 [astro-ph/0202094] [INSPIRE].

[40] L. Boubekeur and D.H. Lyth, *Hilltop inflation*, *JCAP* **07** (2005) 010 [hep-ph/0502047] [INSPIRE].

[41] J. Martin and C. Ringeval, *Inflation after WMAP3: Confronting the Slow-Roll and Exact Power Spectra to CMB Data*, *JCAP* **08** (2006) 009 [astro-ph/0605367] [INSPIRE].

[42] I. Moss and C. Graham, *Testing models of inflation with CMB non-gaussianity*, *JCAP* **11** (2007) 004 [arXiv:0707.1647] [INSPIRE].

[43] F. Bezrukov, A. Magnin, M. Shaposhnikov and S. Sibiryakov, *Higgs inflation: consistency and generalisations*, *JHEP* **01** (2011) 016 [arXiv:1008.5157] [INSPIRE].

[44] W. Zhao and Q.-G. Huang, *Testing inflationary consistency relations by the potential CMB observations*, *Class. Quant. Grav.* **28** (2011) 235003 [arXiv:1101.3163] [INSPIRE].

[45] J. Martin, C. Ringeval and V. Vennin, *How Well Can Future CMB Missions Constrain Cosmic Inflation?*, *JCAP* **10** (2014) 038 [arXiv:1407.4034] [INSPIRE].

[46] J. Martin, C. Ringeval, R. Trotta and V. Vennin, *Compatibility of Planck and BICEP2 in the Light of Inflation*, *Phys. Rev. D* **90** (2014) 063501 [arXiv:1405.7272] [INSPIRE].

[47] M. Carrillo-González, G. Germán-Velarde, A. Herrera-Aguilar, J.C. Hidalgo and R. Sussman, *Testing Hybrid Natural Inflation with BICEP2*, *Phys. Lett. B* **734** (2014) 345 [arXiv:1404.1122] [INSPIRE].

JCAP12(2023)014

[48] P. Creminelli, D. López Nacir, M. Simonović, G. Trevisan and M. Zaldarriaga, ϕ^2 *or Not* ϕ^2*: Testing the Simplest Inflationary Potential*, *Phys. Rev. Lett.* **112** (2014) 241303 [arXiv:1404.1065] [INSPIRE].

[49] E. Di Valentino and L. Mersini-Houghton, *Testing Predictions of the Quantum Landscape Multiverse 1: The Starobinsky Inflationary Potential*, *JCAP* **03** (2017) 002 [arXiv:1612.09588] [INSPIRE].

[50] E. Di Valentino and L. Mersini-Houghton, *Testing Predictions of the Quantum Landscape Multiverse 2: The Exponential Inflationary Potential*, *JCAP* **03** (2017) 020 [arXiv:1612.08334] [INSPIRE].

[51] M. Campista, M. Benetti and J. Alcaniz, *Testing non-minimally coupled inflation with CMB data: a Bayesian analysis*, *JCAP* **09** (2017) 010 [arXiv:1705.08877] [INSPIRE].

[52] W. Giarè, E. Di Valentino and A. Melchiorri, *Testing the inflationary slow-roll condition with tensor modes*, *Phys. Rev. D* **99** (2019) 123522 [INSPIRE].

[53] R. Dai and Y. Zhu, *Testing kinetically coupled inflation models with CMB distortions*, *JCAP* **05** (2020) 017 [arXiv:1911.05973] [INSPIRE].

[54] D. Baumann, H. Lee and G.L. Pimentel, *High-Scale Inflation and the Tensor Tilt*, *JHEP* **01** (2016) 101 [arXiv:1507.07250] [INSPIRE].

[55] S.D. Odintsov, V.K. Oikonomou and F.P. Fronimos, *Canonical scalar field inflation with string and* R^2 *-corrections*, *Annals Phys.* **424** (2021) 168359 [arXiv:2011.08680] [INSPIRE].

[56] W. Giarè, F. Renzi and A. Melchiorri, *Higher-Curvature Corrections and Tensor Modes*, *Phys. Rev. D* **103** (2021) 043515 [arXiv:2012.00527] [INSPIRE].

[57] V.K. Oikonomou, *A refined Einstein-Gauss-Bonnet inflationary theoretical framework*, *Class. Quant. Grav.* **38** (2021) 195025 [arXiv:2108.10460] [INSPIRE].

[58] S.D. Odintsov, V.K. Oikonomou and R. Myrzakulov, *Spectrum of Primordial Gravitational Waves in Modified Gravities: A Short Overview*, *Symmetry* **14** (2022) 729 [arXiv:2204.00876] [INSPIRE].

[59] R. Namba, M. Peloso, M. Shiraishi, L. Sorbo and C. Unal, *Scale-dependent gravitational waves from a rolling axion*, *JCAP* **01** (2016) 041 [arXiv:1509.07521] [INSPIRE].

[60] M. Peloso, L. Sorbo and C. Unal, *Rolling axions during inflation: perturbativity and signatures*, *JCAP* **09** (2016) 001 [arXiv:1606.00459] [INSPIRE].

[61] S. Pi, M. Sasaki and Y.-l. Zhang, *Primordial Tensor Perturbation in Double Inflationary Scenario with a Break*, *JCAP* **06** (2019) 049 [arXiv:1904.06304] [INSPIRE].

[62] O. Özsoy, *Synthetic Gravitational Waves from a Rolling Axion Monodromy*, *JCAP* **04** (2021) 040 [arXiv:2005.10280] [INSPIRE].

[63] A. Stewart and R. Brandenberger, *Observational Constraints on Theories with a Blue Spectrum of Tensor Modes*, *JCAP* **08** (2008) 012 [arXiv:0711.4602] [INSPIRE].

[64] S. Mukohyama, R. Namba, M. Peloso and G. Shiu, *Blue Tensor Spectrum from Particle Production during Inflation*, *JCAP* **08** (2014) 036 [arXiv:1405.0346] [INSPIRE].

[65] M. Giovannini, *The refractive index of relic gravitons*, *Class. Quant. Grav.* **33** (2016) 125002 [arXiv:1507.03456] [INSPIRE].

[66] M. Giovannini, *Post-inflationary thermal histories and the refractive index of relic gravitons*, *Phys. Rev. D* **98** (2018) 103509 [arXiv:1806.01937] [INSPIRE].

[67] M. Giovannini, *Blue and violet graviton spectra from a dynamical refractive index*, *Phys. Lett. B* **789** (2019) 502 [arXiv:1805.08142] [INSPIRE].

[68] M. Giovannini, *The propagating speed of relic gravitational waves and their refractive index during inflation*, *Eur. Phys. J. C* **78** (2018) 442 [arXiv:1803.05203] [INSPIRE].

JCAP12(2023)014

[69] W. Giarè and A. Melchiorri, *Probing the inflationary background of gravitational waves from large to small scales*, *Phys. Lett. B* **815** (2021) 136137 [arXiv:2003.04783] [INSPIRE].

[70] W. Giarè and F. Renzi, *Propagating speed of primordial gravitational waves*, *Phys. Rev. D* **102** (2020) 083530 [arXiv:2007.04256] [INSPIRE].

[71] W. Giarè, M. Forconi, E. Di Valentino and A. Melchiorri, *Towards a reliable calculation of relic radiation from primordial gravitational waves*, *Mon. Not. Roy. Astron. Soc.* **520** (2023) 2 [arXiv:2210.14159] [INSPIRE].

[72] M. Baumgart, J.J. Heckman and L. Thomas, *CFTs blueshift tensor fluctuations universally*, *JCAP* **07** (2022) 034 [arXiv:2109.08166] [INSPIRE].

[73] G. Franciolini, G.F. Giudice, D. Racco and A. Riotto, *Implications of the detection of primordial gravitational waves for the Standard Model*, *JCAP* **05** (2019) 022 [arXiv:1811.08118] [INSPIRE].

[74] F. D'Eramo and K. Schmitz, *Imprint of a scalar era on the primordial spectrum of gravitational waves*, *Phys. Rev. Res.* **1** (2019) 013010 [arXiv:1904.07870] [INSPIRE].

[75] R.R. Caldwell, T.L. Smith and D.G.E. Walker, *Using a Primordial Gravitational Wave Background to Illuminate New Physics*, *Phys. Rev. D* **100** (2019) 043513 [arXiv:1812.07577] [INSPIRE].

[76] T.J. Clarke, E.J. Copeland and A. Moss, *Constraints on primordial gravitational waves from the Cosmic Microwave Background*, *JCAP* **10** (2020) 002 [arXiv:2004.11396] [INSPIRE].

[77] C. Caprini and D.G. Figueroa, *Cosmological Backgrounds of Gravitational Waves*, *Class. Quant. Grav.* **35** (2018) 163001 [arXiv:1801.04268] [INSPIRE].

[78] B. Allen and J.D. Romano, *Detecting a stochastic background of gravitational radiation: Signal processing strategies and sensitivities*, *Phys. Rev. D* **59** (1999) 102001 [gr-qc/9710117] [INSPIRE].

[79] T.L. Smith, E. Pierpaoli and M. Kamionkowski, *A new cosmic microwave background constraint to primordial gravitational waves*, *Phys. Rev. Lett.* **97** (2006) 021301 [astro-ph/0603144] [INSPIRE].

[80] L.A. Boyle and A. Buonanno, *Relating gravitational wave constraints from primordial nucleosynthesis, pulsar timing, laser interferometers, and the CMB: Implications for the early Universe*, *Phys. Rev. D* **78** (2008) 043531 [arXiv:0708.2279] [INSPIRE].

[81] S. Kuroyanagi, T. Takahashi and S. Yokoyama, *Blue-tilted Tensor Spectrum and Thermal History of the Universe*, *JCAP* **02** (2015) 003 [arXiv:1407.4785] [INSPIRE].

[82] I. Ben-Dayan, B. Keating, D. Leon and I. Wolfson, *Constraints on scalar and tensor spectra from N_{eff}*, *JCAP* **06** (2019) 007 [arXiv:1903.11843] [INSPIRE].

[83] M. Aich, Y.-Z. Ma, W.-M. Dai and J.-Q. Xia, *How much primordial tensor mode is allowed?*, *Phys. Rev. D* **101** (2020) 063536 [arXiv:1912.00995] [INSPIRE].

[84] G. Cabass, L. Pagano, L. Salvati, M. Gerbino, E. Giusarma and A. Melchiorri, *Updated Constraints and Forecasts on Primordial Tensor Modes*, *Phys. Rev. D* **93** (2016) 063508 [arXiv:1511.05146] [INSPIRE].

[85] S. Vagnozzi, *Implications of the NANOGrav results for inflation*, *Mon. Not. Roy. Astron. Soc.* **502** (2021) L11 [arXiv:2009.13432] [INSPIRE].

[86] M. Benetti, L.L. Graef and S. Vagnozzi, *Primordial gravitational waves from NANOGrav: A broken power-law approach*, *Phys. Rev. D* **105** (2022) 043520 [arXiv:2111.04758] [INSPIRE].

[87] G. Calcagni and S. Kuroyanagi, *Stochastic gravitational-wave background in quantum gravity*, *JCAP* **03** (2021) 019 [arXiv:2012.00170] [INSPIRE].

JCAP12(2023)014

[88] V.K. Oikonomou, *Amplification of the Primordial Gravitational Waves Energy Spectrum by a Kinetic Scalar in $F(R)$ Gravity*, *Astropart. Phys.* **144** (2023) 102777 [arXiv:2209.09781] [INSPIRE].

[89] J.D. Barrow, J.P. Mimoso and M.R. de Garcia Maia, *Amplification of gravitational waves in scalar-tensor theories of gravity*, *Phys. Rev. D* **48** (1993) 3630 [*Erratum ibid.* **51** (1995) 5967] [INSPIRE].

[90] Z.-Z. Peng, C. Fu, J. Liu, Z.-K. Guo and R.-G. Cai, *Gravitational waves from resonant amplification of curvature perturbations during inflation*, *JCAP* **10** (2021) 050 [arXiv:2106.11816] [INSPIRE].

[91] A. Ota, M. Sasaki and Y. Wang, *Scale-invariant enhancement of gravitational waves during inflation*, *Mod. Phys. Lett. A* **38** (2023) 2350063 [arXiv:2209.02272] [INSPIRE].

[92] S.D. Odintsov and V.K. Oikonomou, *Amplification of Primordial Gravitational Waves by a Geometrically Driven non-canonical Reheating Era*, *Fortsch. Phys.* **70** (2022) 2100167 [arXiv:2203.10599] [INSPIRE].

[93] G. Capurri, N. Bartolo, D. Maino and S. Matarrese, *Let Effective Field Theory of Inflation flow: stochastic generation of models with red/blue tensor tilt*, *JCAP* **11** (2020) 037 [arXiv:2006.10781] [INSPIRE].

[94] G. Cañas Herrera and F. Renzi, *Current and future constraints on single-field α-attractor models*, *Phys. Rev. D* **104** (2021) 103512 [arXiv:2104.06398] [INSPIRE].

[95] S.D. Odintsov, V.K. Oikonomou and F.P. Fronimos, *Inflationary Dynamics and Swampland Criteria for Modified Gauss-Bonnet Gravity Compatible with GW170817*, *Phys. Rev. D* **107** (2023) 08 [arXiv:2303.14594] [INSPIRE].

[96] V.K. Oikonomou, *Effects of the axion through the Higgs portal on primordial gravitational waves during the electroweak breaking*, *Phys. Rev. D* **107** (2023) 064071 [arXiv:2303.05889] [INSPIRE].

[97] F.P. Fronimos and S.A. Venikoudis, *Inflationary phenomenology of non-minimally coupled Einstein-Chern-Simons gravity*, *Eur. Phys. J. Plus* **138** (2023) 529 [arXiv:2302.05173] [INSPIRE].

[98] Y. Cai, *Generating enhanced parity-violating gravitational waves during inflation with violation of the null energy condition*, *Phys. Rev. D* **107** (2023) 063512 [arXiv:2212.10893] [INSPIRE].

[99] V.K. Oikonomou, *Effects of a pre-inflationary de Sitter bounce on the primordial gravitational waves in $f(R)$ gravity theories*, *Nucl. Phys. B* **984** (2022) 115985 [arXiv:2210.02861] [INSPIRE].

[100] M.R. Gangopadhyay, H.A. Khan and Yogesh, *A case study of small field inflationary dynamics in the Einstein-Gauss-Bonnet framework in the light of GW170817*, *Phys. Dark Univ.* **40** (2023) 101177 [arXiv:2205.15261] [INSPIRE].

[101] S.D. Odintsov and V.K. Oikonomou, *Chirality of gravitational waves in Chern-Simons $f(R)$ gravity cosmology*, *Phys. Rev. D* **105** (2022) 104054 [arXiv:2205.07304] [INSPIRE].

[102] S.D. Odintsov, V.K. Oikonomou, F.P. Fronimos and S.A. Venikoudis, *GW170817-compatible constant-roll Einstein-Gauss-Bonnet inflation and non-Gaussianities*, *Phys. Dark Univ.* **30** (2020) 100718 [arXiv:2009.06113] [INSPIRE].

[103] G. Galloni, N. Bartolo, S. Matarrese, M. Migliaccio, A. Ricciardone and N. Vittorio, *Updated constraints on amplitude and tilt of the tensor primordial spectrum*, *JCAP* **04** (2023) 062 [arXiv:2208.00188] [INSPIRE].

[104] M. De Angelis, L. Figurato and G. Montani, *Quantum dynamics of the isotropic universe in metric $f(R)$ gravity*, *Phys. Rev. D* **104** (2021) 024054 [arXiv:2105.02934] [INSPIRE].

JCAP12(2023)014

[105] R. Kallosh and A. Linde, *Hybrid cosmological attractors*, *Phys. Rev. D* **106** (2022) 023522 [arXiv:2204.02425] [INSPIRE].

[106] M. Braglia, A. Linde, R. Kallosh and F. Finelli, *Hybrid α-attractors, primordial black holes and gravitational wave backgrounds*, *JCAP* **04** (2023) 033 [arXiv:2211.14262] [INSPIRE].

[107] S. Vagnozzi and A. Loeb, *The Challenge of Ruling Out Inflation via the Primordial Graviton Background*, *Astrophys. J. Lett.* **939** (2022) L22 [arXiv:2208.14088] [INSPIRE].

[108] L. Senatore and M. Zaldarriaga, *The Effective Field Theory of Multifield Inflation*, *JHEP* **04** (2012) 024 [arXiv:1009.2093] [INSPIRE].

[109] A.A. Starobinsky, S. Tsujikawa and J. Yokoyama, *Cosmological perturbations from multifield inflation in generalized Einstein theories*, *Nucl. Phys. B* **610** (2001) 383 [astro-ph/0107555] [INSPIRE].

[110] S. Tsujikawa, D. Parkinson and B.A. Bassett, *Correlation-consistency cartography of the double inflation landscape*, *Phys. Rev. D* **67** (2003) 083516 [astro-ph/0210322] [INSPIRE].

[111] F. Di Marco, F. Finelli and R. Brandenberger, *Adiabatic and isocurvature perturbations for multifield generalized Einstein models*, *Phys. Rev. D* **67** (2003) 063512 [astro-ph/0211276] [INSPIRE].

[112] D.I. Kaiser, *Conformal Transformations with Multiple Scalar Fields*, *Phys. Rev. D* **81** (2010) 084044 [arXiv:1003.1159] [INSPIRE].

[113] A. Achucarro, J.-O. Gong, S. Hardeman, G.A. Palma and S.P. Patil, *Features of heavy physics in the CMB power spectrum*, *JCAP* **01** (2011) 030 [arXiv:1010.3693] [INSPIRE].

[114] C. van de Bruck, D.F. Mota and J.M. Weller, *Embedding DBI inflation in scalar-tensor theory*, *JCAP* **03** (2011) 034 [arXiv:1012.1567] [INSPIRE].

[115] D.I. Kaiser and E.I. Sfakianakis, *Multifield Inflation after Planck: The Case for Nonminimal Couplings*, *Phys. Rev. Lett.* **112** (2014) 011302 [arXiv:1304.0363] [INSPIRE].

[116] C. van de Bruck, T. Koivisto and C. Longden, *Disformally coupled inflation*, *JCAP* **03** (2016) 006 [arXiv:1510.01650] [INSPIRE].

[117] C. van de Bruck and L.E. Paduraru, *Simplest extension of Starobinsky inflation*, *Phys. Rev. D* **92** (2015) 083513 [arXiv:1505.01727] [INSPIRE].

[118] C. van de Bruck, T. Koivisto and C. Longden, *Non-Gaussianity in multi-sound-speed disformally coupled inflation*, *JCAP* **02** (2017) 029 [arXiv:1608.08801] [INSPIRE].

[119] P. Carrilho, D. Mulryne, J. Ronayne and T. Tenkanen, *Attractor Behaviour in Multifield Inflation*, *JCAP* **06** (2018) 032 [arXiv:1804.10489] [INSPIRE].

[120] A. Achúcarro, E.J. Copeland, O. Iarygina, G.A. Palma, D.-G. Wang and Y. Welling, *Shift-symmetric orbital inflation: Single field or multifield?*, *Phys. Rev. D* **102** (2020) 021302 [arXiv:1901.03657] [INSPIRE].

[121] L. Pinol, *Multifield inflation beyond $N_{\rm field} = 2$: non-Gaussianities and single-field effective theory*, *JCAP* **04** (2021) 002 [arXiv:2011.05930] [INSPIRE].

[122] A. Achúcarro and G.A. Palma, *The string swampland constraints require multi-field inflation*, *JCAP* **02** (2019) 041 [arXiv:1807.04390] [INSPIRE].

[123] C. van de Bruck and R. Daniel, *Inflation and scale-invariant R^2 gravity*, *Phys. Rev. D* **103** (2021) 123506 [arXiv:2102.11719] [INSPIRE].

[124] M. De Angelis and C. van de Bruck, *Adiabatic and isocurvature perturbations in extended theories with kinetic couplings*, *JCAP* **10** (2023) 023 [arXiv:2304.12364] [INSPIRE].

[125] S. Weinberg, *Must cosmological perturbations remain non-adiabatic after multi-field inflation?*, *Phys. Rev. D* **70** (2004) 083522 [astro-ph/0405397] [INSPIRE].

JCAP12(2023)014

[126] S. Tsujikawa and H. Yajima, *New constraints on multifield inflation with nonminimal coupling*, *Phys. Rev. D* **62** (2000) 123512 [hep-ph/0007351] [INSPIRE].

[127] D.I. Kaiser and A.T. Todhunter, *Primordial Perturbations from Multifield Inflation with Nonminimal Couplings*, *Phys. Rev. D* **81** (2010) 124037 [arXiv:1004.3805] [INSPIRE].

[128] J. Frazer, *Predictions in multifield models of inflation*, *JCAP* **01** (2014) 028 [arXiv:1303.3611] [INSPIRE].

[129] A. Achúcarro, J.-O. Gong, G.A. Palma and S.P. Patil, *Correlating features in the primordial spectra*, *Phys. Rev. D* **87** (2013) 121301 [arXiv:1211.5619] [INSPIRE].

[130] C. van de Bruck and M. Robinson, *Power Spectra beyond the Slow Roll Approximation in Theories with Non-Canonical Kinetic Terms*, *JCAP* **08** (2014) 024 [arXiv:1404.7806] [INSPIRE].

[131] M. Dias, J. Frazer and D. Seery, *Computing observables in curved multifield models of inflation — A guide (with code) to the transport method*, *JCAP* **12** (2015) 030 [arXiv:1502.03125] [INSPIRE].

[132] M. Dias, J. Frazer, D.J. Mulryne and D. Seery, *Numerical evaluation of the bispectrum in multiple field inflation — the transport approach with code*, *JCAP* **12** (2016) 033 [arXiv:1609.00379] [INSPIRE].

[133] M. Braglia, D.K. Hazra, L. Sriramkumar and F. Finelli, *Generating primordial features at large scales in two field models of inflation*, *JCAP* **08** (2020) 025 [arXiv:2004.00672] [INSPIRE].

[134] M. Braglia, X. Chen and D.K. Hazra, *Comparing multi-field primordial feature models with the Planck data*, *JCAP* **06** (2021) 005 [arXiv:2103.03025] [INSPIRE].

[135] G. Cabass, M.M. Ivanov, O.H.E. Philcox, M. Simonović and M. Zaldarriaga, *Constraints on multifield inflation from the BOSS galaxy survey*, *Phys. Rev. D* **106** (2022) 043506 [arXiv:2204.01781] [INSPIRE].

[136] S.R. Geller, W. Qin, E. McDonough and D.I. Kaiser, *Primordial black holes from multifield inflation with nonminimal couplings*, *Phys. Rev. D* **106** (2022) 063535 [arXiv:2205.04471] [INSPIRE].

[137] D.-G. Wang, G.L. Pimentel and A. Achúcarro, *Bootstrapping multi-field inflation: non-Gaussianities from light scalars revisited*, *JCAP* **05** (2023) 043 [arXiv:2212.14035] [INSPIRE].

[138] L. Iacconi and D.J. Mulryne, *Multi-field inflation with large scalar fluctuations: non-Gaussianity and perturbativity*, *JCAP* **09** (2023) 033 [arXiv:2304.14260] [INSPIRE].

[139] W. Qin, S.R. Geller, S. Balaji, E. McDonough and D.I. Kaiser, *Planck constraints and gravitational wave forecasts for primordial black hole dark matter seeded by multifield inflation*, *Phys. Rev. D* **108** (2023) 043508 [arXiv:2303.02168] [INSPIRE].

[140] M. Freytsis, S. Kumar, G.N. Remmen and N.L. Rodd, *Multifield positivity bounds for inflation*, *JHEP* **09** (2023) 041 [arXiv:2210.10791] [INSPIRE].

[141] M. Cicoli, V. Guidetti, F. Muia, F.G. Pedro and G.P. Vacca, *On the choice of entropy variables in multifield inflation*, *Class. Quant. Grav.* **40** (2023) 025008 [arXiv:2107.03391] [INSPIRE].

[142] M. Guerrero, D. Rubiera-Garcia and D. Saez-Chillon Gomez, *Constant roll inflation in multifield models*, *Phys. Rev. D* **102** (2020) 123528 [arXiv:2008.07260] [INSPIRE].

[143] S. Garcia-Saenz, L. Pinol and S. Renaux-Petel, *Revisiting non-Gaussianity in multifield inflation with curved field space*, *JHEP* **01** (2020) 073 [arXiv:1907.10403] [INSPIRE].

JCAP12(2023)014

[144] R. Nguyen, J. van de Vis, E.I. Sfakianakis, J.T. Giblin and D.I. Kaiser, *Nonlinear Dynamics of Preheating after Multifield Inflation with Nonminimal Couplings*, *Phys. Rev. Lett.* **123** (2019) 171301 [arXiv:1905.12562] [INSPIRE].

[145] X.-B. Li, X.-G. Zheng and J.-Y. Zhu, *Spectra and entropy of multifield warm inflation*, *Phys. Rev. D* **99** (2019) 043528 [arXiv:1902.01017] [INSPIRE].

[146] F. Bernardeau and J.-P. Uzan, *NonGaussianity in multifield inflation*, *Phys. Rev. D* **66** (2002) 103506 [hep-ph/0207295] [INSPIRE].

[147] D.I. Kaiser, E.A. Mazenc and E.I. Sfakianakis, *Primordial Bispectrum from Multifield Inflation with Nonminimal Couplings*, *Phys. Rev. D* **87** (2013) 064004 [arXiv:1210.7487] [INSPIRE].

[148] L. McAllister, S. Renaux-Petel and G. Xu, *A Statistical Approach to Multifield Inflation: Many-field Perturbations Beyond Slow Roll*, *JCAP* **10** (2012) 046 [arXiv:1207.0317] [INSPIRE].

[149] C.M. Peterson and M. Tegmark, *Testing multifield inflation: A geometric approach*, *Phys. Rev. D* **87** (2013) 103507 [arXiv:1111.0927] [INSPIRE].

[150] M. Dias, J. Frazer and A.R. Liddle, *Multifield consequences for D-brane inflation*, *JCAP* **06** (2012) 020 [arXiv:1203.3792] [*Erratum ibid.* **03** (2013) E01] [INSPIRE].

[151] A. Kehagias and A. Riotto, *The Four-point Correlator in Multifield Inflation, the Operator Product Expansion and the Symmetries of de Sitter*, *Nucl. Phys. B* **868** (2013) 577 [arXiv:1210.1918] [INSPIRE].

[152] G. Leung, E.R.M. Tarrant, C.T. Byrnes and E.J. Copeland, *Reheating, Multifield Inflation and the Fate of the Primordial Observables*, *JCAP* **09** (2012) 008 [arXiv:1206.5196] [INSPIRE].

[153] J. Meyers and N. Sivanandam, *Non-Gaussianities in Multifield Inflation: Superhorizon Evolution, Adiabaticity, and the Fate of fnl*, *Phys. Rev. D* **83** (2011) 103517 [arXiv:1011.4934] [INSPIRE].

[154] L.C. Price, H.V. Peiris, J. Frazer and R. Easther, *Gravitational wave consistency relations for multifield inflation*, *Phys. Rev. Lett.* **114** (2015) 031301 [arXiv:1409.2498] [INSPIRE].

[155] D. Battefeld, T. Battefeld, C. Byrnes and D. Langlois, *Beauty is Distractive: Particle production during multifield inflation*, *JCAP* **08** (2011) 025 [arXiv:1106.1891] [INSPIRE].

[156] D.I. Kaiser, *Nonminimal Couplings in the Early Universe: Multifield Models of Inflation and the Latest Observations*, *Fundam. Theor. Phys.* **183** (2016) 41 [arXiv:1511.09148] [INSPIRE].

[157] P.R. Ashcroft, C. van de Bruck and A.C. Davis, *Suppression of entropy perturbations in multi-field inflation on the brane*, *Phys. Rev. D* **66** (2002) 121302 [astro-ph/0208411] [INSPIRE].

[158] A. Paliathanasis and G. Leon, *Global dynamics of the hyperbolic Chiral-Phantom model*, *Eur. Phys. J. Plus* **137** (2022) 165 [arXiv:2105.03261] [INSPIRE].

[159] A. Paliathanasis and G. Leon, *Asymptotic behavior of N-fields Chiral Cosmology*, *Eur. Phys. J. C* **80** (2020) 847 [arXiv:2007.13223] [INSPIRE].

[160] A. Paliathanasis, *Dynamics of Chiral Cosmology*, *Class. Quant. Grav.* **37** (2020) 195014 [arXiv:2003.05342] [INSPIRE].

[161] P. Christodoulidis and A. Paliathanasis, *$\mathcal{N}$-field cosmology in hyperbolic field space: stability and general solutions*, *JCAP* **05** (2021) 038 [arXiv:2101.09582] [INSPIRE].

[162] Y.-S. Piao, *On perturbation spectra of N-flation*, *Phys. Rev. D* **74** (2006) 047302 [gr-qc/0606034] [INSPIRE].

JCAP12(2023)014

[163] M. Rinaldi, C. Cecchini, A. Ghoshal and D. Mukherjee, *Scale-invariant inflation*, *J. Phys. Conf. Ser.* **2531** (2023) 012012 [arXiv:2303.16107] [INSPIRE].

[164] PLANCK collaboration, *Planck 2018 results. VI. Cosmological parameters*, *Astron. Astrophys.* **641** (2020) A6 [arXiv:1807.06209] [*Erratum ibid.* **652** (2021) C4] [INSPIRE].

[165] PLANCK collaboration, *Planck 2018 results. I. Overview and the cosmological legacy of Planck*, *Astron. Astrophys.* **641** (2020) A1 [arXiv:1807.06205] [INSPIRE].

[166] ACT collaboration, *The Atacama Cosmology Telescope: DR4 Maps and Cosmological Parameters*, *JCAP* **12** (2020) 047 [arXiv:2007.07288] [INSPIRE].

[167] ACT collaboration, *The Atacama Cosmology Telescope: a measurement of the Cosmic Microwave Background power spectra at 98 and 150 GHz*, *JCAP* **12** (2020) 045 [arXiv:2007.07289] [INSPIRE].

[168] SPT-3G collaboration, *Measurement of the CMB temperature power spectrum and constraints on cosmology from the SPT-3G 2018 TT, TE, and EE dataset*, *Phys. Rev. D* **108** (2023) 023510 [arXiv:2212.05642] [INSPIRE].

[169] SPT-3G collaboration, *SPT-3G: A Next-Generation Cosmic Microwave Background Polarization Experiment on the South Pole Telescope*, *Proc. SPIE Int. Soc. Opt. Eng.* **9153** (2014) 91531P [arXiv:1407.2973] [INSPIRE].

[170] SPT-3G collaboration, *Measurements of the E-mode polarization and temperature-E-mode correlation of the CMB from SPT-3G 2018 data*, *Phys. Rev. D* **104** (2021) 022003 [arXiv:2101.01684] [INSPIRE].

[171] R. Easther, J. Frazer, H.V. Peiris and L.C. Price, *Simple predictions from multifield inflationary models*, *Phys. Rev. Lett.* **112** (2014) 161302 [arXiv:1312.4035] [INSPIRE].

[172] L.C. Price, J. Frazer, J. Xu, H.V. Peiris and R. Easther, *MultiModeCode: An efficient numerical solver for multifield inflation*, *JCAP* **03** (2015) 005 [arXiv:1410.0685] [INSPIRE].

[173] A. Lewis, A. Challinor and A. Lasenby, *Efficient computation of CMB anisotropies in closed FRW models*, *Astrophys. J.* **538** (2000) 473 [astro-ph/9911177] [INSPIRE].

[174] C. Howlett, A. Lewis, A. Hall and A. Challinor, *CMB power spectrum parameter degeneracies in the era of precision cosmology*, *JCAP* **04** (2012) 027 [arXiv:1201.3654] [INSPIRE].

[175] D. Blas, J. Lesgourgues and T. Tram, *The Cosmic Linear Anisotropy Solving System (CLASS) II: Approximation schemes*, *JCAP* **07** (2011) 034 [arXiv:1104.2933] [INSPIRE].

[176] C. Gordon, D. Wands, B.A. Bassett and R. Maartens, *Adiabatic and entropy perturbations from inflation*, *Phys. Rev. D* **63** (2000) 023506 [astro-ph/0009131] [INSPIRE].

[177] F. Di Marco, F. Finelli and R. Brandenberger, *Adiabatic and isocurvature perturbations for multifield generalized Einstein models*, *Phys. Rev. D* **67** (2003) 063512 [astro-ph/0211276] [INSPIRE].

[178] D. Langlois and S. Renaux-Petel, *Perturbations in generalized multi-field inflation*, *JCAP* **04** (2008) 017 [arXiv:0801.1085] [INSPIRE].

[179] D. Wands, N. Bartolo, S. Matarrese and A. Riotto, *An Observational test of two-field inflation*, *Phys. Rev. D* **66** (2002) 043520 [astro-ph/0205253] [INSPIRE].

[180] J. Silk and M.S. Turner, *Double Inflation*, *Phys. Rev. D* **35** (1987) 419 [INSPIRE].

[181] D. Polarski and A.A. Starobinsky, *Spectra of perturbations produced by double inflation with an intermediate matter dominated stage*, *Nucl. Phys. B* **385** (1992) 623 [INSPIRE].

[182] D. Roberts, A.R. Liddle and D.H. Lyth, *False vacuum inflation with a quartic potential*, *Phys. Rev. D* **51** (1995) 4122 [astro-ph/9411104] [INSPIRE].

[183] D. Langlois, *Correlated adiabatic and isocurvature perturbations from double inflation*, *Phys. Rev. D* **59** (1999) 123512 [astro-ph/9906080] [INSPIRE].

JCAP12(2023)014

[184] S.M. Leach and A.R. Liddle, *Inflationary perturbations near horizon crossing*, *Phys. Rev. D* **63** (2001) 043508 [astro-ph/0010082] [INSPIRE].

[185] S.M. Leach, M. Sasaki, D. Wands and A.R. Liddle, *Enhancement of superhorizon scale inflationary curvature perturbations*, *Phys. Rev. D* **64** (2001) 023512 [astro-ph/0101406] [INSPIRE].

[186] R.K. Jain, P. Chingangbam and L. Sriramkumar, *On the evolution of tachyonic perturbations at super-Hubble scales*, *JCAP* **10** (2007) 003 [astro-ph/0703762] [INSPIRE].

[187] R.K. Jain, P. Chingangbam, J.-O. Gong, L. Sriramkumar and T. Souradeep, *Punctuated inflation and the low CMB multipoles*, *JCAP* **01** (2009) 009 [arXiv:0809.3915] [INSPIRE].

[188] R.K. Jain, P. Chingangbam, L. Sriramkumar and T. Souradeep, *The tensor-to-scalar ratio in punctuated inflation*, *Phys. Rev. D* **82** (2010) 023509 [arXiv:0904.2518] [INSPIRE].

[189] R. Kallosh, A. Linde and D. Roest, *Large field inflation and double α-attractors*, *JHEP* **08** (2014) 052 [arXiv:1405.3646] [INSPIRE].

[190] H.V. Ragavendra, D. Chowdhury and L. Sriramkumar, *Suppression of scalar power on large scales and associated bispectra*, *Phys. Rev. D* **106** (2022) 043535 [arXiv:2003.01099] [INSPIRE].

[191] Planck collaboration, *Planck 2018 results. V. CMB power spectra and likelihoods*, *Astron. Astrophys.* **641** (2020) A5 [arXiv:1907.12875] [INSPIRE].

[192] Planck collaboration, *Planck 2018 results. VI. Cosmological parameters*, *Astron. Astrophys.* **641** (2020) A6 [arXiv:1807.06209] [*Erratum ibid.* **652** (2021) C4] [INSPIRE].

[193] Planck collaboration, *Planck 2018 results. I. Overview and the cosmological legacy of Planck*, *Astron. Astrophys.* **641** (2020) A1 [arXiv:1807.06205] [INSPIRE].

[194] Planck collaboration, *Planck 2018 results. VIII. Gravitational lensing*, *Astron. Astrophys.* **641** (2020) A8 [arXiv:1807.06210] [INSPIRE].

[195] J.M. Bardeen, *Gauge Invariant Cosmological Perturbations*, *Phys. Rev. D* **22** (1980) 1882 [INSPIRE].

[196] C. van de Bruck and C. Longden, *Running of the Running and Entropy Perturbations During Inflation*, *Phys. Rev. D* **94** (2016) 021301 [arXiv:1606.02176] [INSPIRE].

[197] X. Chen and C. Ringeval, *Searching for Standard Clocks in the Primordial Universe*, *JCAP* **08** (2012) 014 [arXiv:1205.6085] [INSPIRE].

[198] X. Chen and M.H. Namjoo, *Standard Clock in Primordial Density Perturbations and Cosmic Microwave Background*, *Phys. Lett. B* **739** (2014) 285 [arXiv:1404.1536] [INSPIRE].

[199] X. Chen, M.H. Namjoo and Y. Wang, *Models of the Primordial Standard Clock*, *JCAP* **02** (2015) 027 [arXiv:1411.2349] [INSPIRE].

[200] X. Chen, M.H. Namjoo and Y. Wang, *Quantum Primordial Standard Clocks*, *JCAP* **02** (2016) 013 [arXiv:1509.03930] [INSPIRE].

[201] C.M. Peterson and M. Tegmark, *Testing Two-Field Inflation*, *Phys. Rev. D* **83** (2011) 023522 [arXiv:1005.4056] [INSPIRE].

[202] J. Torrado and A. Lewis, *Cobaya: Code for Bayesian Analysis of hierarchical physical models*, *JCAP* **05** (2021) 057 [arXiv:2005.05290] [INSPIRE].

[203] A. Lewis and S. Bridle, *Cosmological parameters from CMB and other data: A Monte Carlo approach*, *Phys. Rev. D* **66** (2002) 103511 [astro-ph/0205436] [INSPIRE].

[204] R.M. Neal, *Taking Bigger Metropolis Steps by Dragging Fast Variables*, math/0502099.

JCAP12(2023)014